Electronic supplementary materials *Mendeleev Commun.*, 2023, **33**, 543–545

Novel sulfonamide-functionalized arylidene indolones as potent α-glucosidase inhibitors: synthesis, characterization, and *in vitro* and *in silico* studies

Giang V. Nguyen, Hoang T. Dang, Luyen D. Nguyen, Hai V. Nguyen, Huong T. Le, Huy H. N. Nguyen, An V. Nguyen, Yen H. Nguyen, Van-Ha Nguyen and Huy-Hoang Do

1. General information

All the melting points were taken in open capillaries device (EZ-Melt, USA). Mass spectra were obtained on a Shimadzu spectrometer. ^{1}H & ^{13}C NMR spectra were obtained on a Bruker 500 MHz Ascend instrument using $CDCl_3$ and DMSO-d_6 as solvent.

2. General procedures

*a) Synthesis of 1-(2,6-dichlorophenyl)indolin-2-one **1***

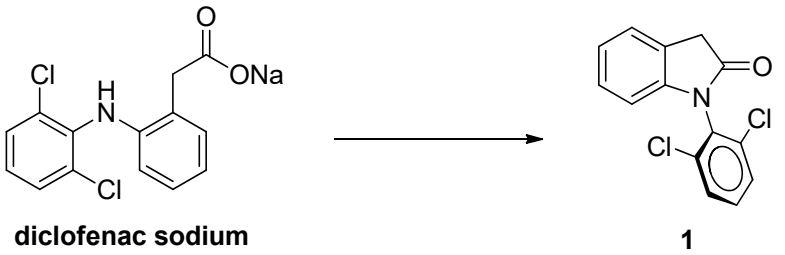

diclofenac sodium **1**

Scheme S1. diluted H_2SO_4

Compound **1** was prepared in 95% yield as previously reported.[S1]

*b) Synthesis of 1-(2,6-dichlorophenyl)-3-arylideneindolin-2-ones **2a-f***

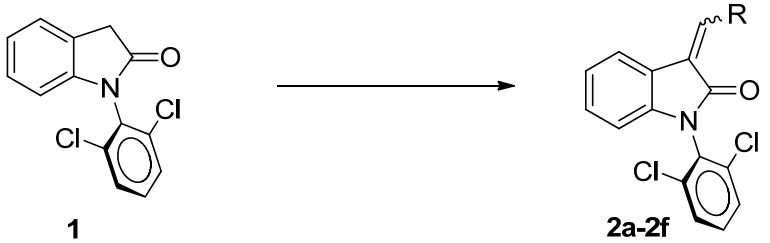

1 **2a-2f**

Scheme S2. RCHO, piperazine, 80 °C, EtOH

In a 50 mL reaction flask, 1-(2,6-dichlorophenyl)indolin-2-one **1** (1.0 mmol) and piperazine (0.37 mmol) were dissolved in ethanol and followed by aldehyde (1.5 mmol). The reaction mixture was refluxed for 24 h. The precipitate was washed with water and recrystallized with ethanol to obtain the pure product **2a-f**.

*c) Synthesis of 5-chlorosulfonyl-1-(2,6-dichlorophenyl)-2-oxoindoline **3***

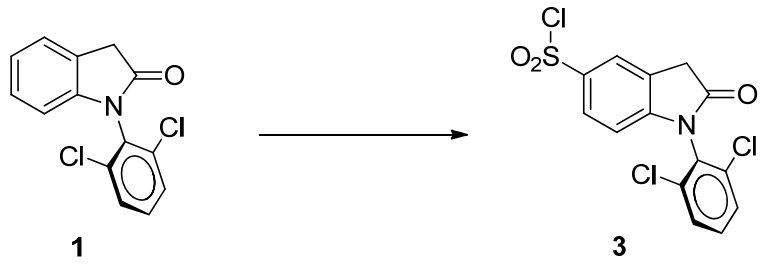

Scheme S3. $ClSO_3H$, 0→20 °C.

In a dried 50 mL reaction flask, chlorosulfonic acid $ClSO_3H$ (10 mL) purged with nitrogen gas was added. The flask was cooled in an ice bath, and 1-(2,6-diclorophenyl)indolin-2-one **1** (0.8 mmol, 222 mg) was added slowly. Then the reaction mixture was stirred for 6 h. Upon completion, the reaction was poured into ice water and the precipitate formed was collected by vacuum filtration and rinsed with water to obtain the pure pink solid **3** (98%). M.p = 243.5-245.4 ºC.

*d) Synthesis of 1-(2,6-dichlorophenyl)-5-methylaminosulfonyl-2-oxoindoline **4***

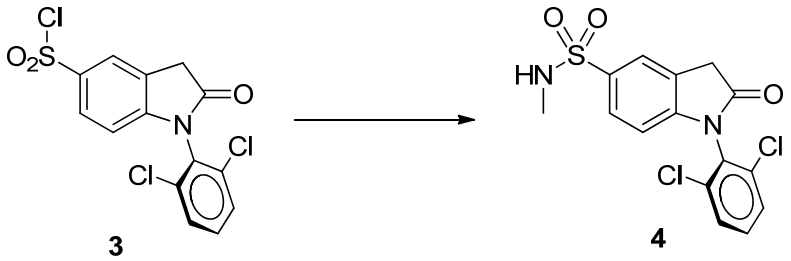

Scheme S4. CH_3NH_2, CH_2Cl_2

In a 50 mL reaction flask, 5-chlorosulfonyl-1-(2,6-dichlorophenyl)-2-oxoindoline **3** (1.0 mmol, 376 mg) was dissolved in dichloromethane. Methylamine (40% wt aqueous solution, 0.12 mL, 1.1 mmol) was added, and this was stirred for 15 minutes. The reaction mixture was concentrated *in vacuo* and the crude residue was triturated with diethyl ether to give pure compound **4** (90%) as a pink solid. M.p = 219.8-221.4 ºC

*e) Synthesis of 3-arylidene-1-(2,6-dichlorophenyl)- 5-(methylaminosulfonyl)indolin-2-ones **5a-f***

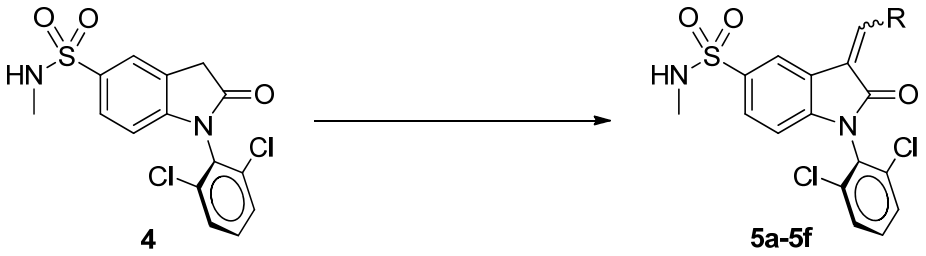

Scheme S5. RCHO, piperazine, 80 °C, EtOH

In a 50 mL reaction flask, 1-(2,6-dichlorophenyl)-5-(methylaminosulfonyl)indolin-2-one **4** (1.0 mmol) and piperazine (0.37 mmol) were dissolved in ethanol, and aldehyde (1.5 mmol) was added. The reaction mixture was refluxed for 24 h. The precipitate product was filtered and rinsed with ethanol, then water to obtain the pure product **5a-f**.

Synthesis of 3-arylidene-1-(2,6-dichlorophenyl)indolin-2-ones 2a-f

In a 50 mL reaction flask, 1-(2,6-dichlorophenyl)indolin-2-one **1** (1.0 mmol) and piperazine (0.37 mmol) were dissolved in ethanol, and aldehyde (1.5 mmol) was added. The reaction mixture was refluxed for 24 h. The precipitate was washed with water and recrystallized with ethanol to obtain the pure product **2a-f**.

2a: Yellow powder, yield 84% (0.11 g). M.p = 133.0 – 133.8 ^{o}C. ^{1}H-NMR ($CDCl_3$, 500 MHz): δ 8.01(s, 1 H, CH=C), 7.78-7.75 (m, 3 H, Ar-H), 7.57-7,48 (m, 5 H, Ar-H), 7.42 (t, 1 H, J = 8.0 Hz, Ar-H), 7.23 (t, 1 H, J = 7.7 Hz, Ar-H), 6.98 (t, 1 H, J = 7.7 Hz, Ar-H), 6.45 (d, 1 H, J = 7.7 Hz, Ar-H). ^{13}C-NMR ($CDCl_3$, 125.77 MHz): δ 167.11 (C=O), 142.28, 138.58, 135.82, 134.82, 130.76, 130.58, 129.86, 129.80, 129.40, 129.05, 128.72, 126.41, 123.13, 122.56, 121.25, 109.31. Mass spectrum, *m/z*: 366.0450 [M+H]$^{+}$. Calcd for $C_{21}H_{14}Cl_2NO$. 366.0452.

2b: Yellow powder, yield 76% (0.11 g). M.p = 140.2–143.5 ^{o}C. ^{1}H-NMR ($CDCl_3$, 500 MHz): δ 7.92 (s, 1 H, C*H*=C), 7.72-7.68 (dd, 3 H, Ar-H), 7.56 (d, 2 H, J = 8.1 Hz, Ar-H), 7.51 (d, 2 H, J = 8.4 Hz, Ar-H), 7.43 (t, 1 H, Ar-H), 7.24 (t, 1 H, J = 7.7 Hz, Ar-H), 6.99 (t, 1 H, J = 7.7 Hz, Ar-H), 6.45 (dd, 1 H, J = 7.9 Hz, Ar-H). ^{13}C-NMR ($CDCl_3$, 125.77 MHz): δ 166.89 (C=O), 142.41, 136.87 (Ar-C), 135.78, 135.69 (C=C), 133.54, 133.26, 130.81, 130.72, 130.14, 129.06, 128.59, 126.89, 123.06, 122.65, 120.96, 109.46 (Ar-C). Mass spectrum, *m/z*: 400.0065 [M+H]$^{+}$. Calcd for $C_{21}H_{13}Cl_3NO$. 400.0063.

2c: Pale yellow powder, yield 68% (0.10 g). M.p = 175.1–178.3 ^{o}C. ^{1}H-NMR ($CDCl_3$, 500 MHz): δ 9.02 (s, 1 H, $H^{2'}$), 8.71 (d, 1 H, J = 7.9 Hz, $H^{6'}$), 8.26 – 8.24 (dd, 1 H, J = 8.2 Hz, H^{4}), 7.68 (d, 1 H, J = 7.3 Hz, Ar-H), 7.68 (s, 1 H, CH=C), 7.60 (t, 1 H, J = 8.0 Hz, Ar-H),

7.53 (d, 1 H, *J* = 8.1 Hz, Ar-H), 7.40 (t, 1 H, *J* = 8.0 Hz, Ar-H), 7.29 (d, 1 H, J = 7.4 Hz, Ar-H), 7.17 (t, 1 H, *J* = 7.4 Hz, Ar-H), 6.45 (d, 1 H, *J* = 7.8 Hz, Ar-H). ^{13}C-NMR ($CDCl_3$, 125.77 MHz): δ 164.50 (C=O), 141.14, 137.30, 135.76, 134.98, 130.90, 129.22, 127.94, 126.52, 124.73, 123.62, 122.99, 121.93, 119.97, 119.23, 109.36. Mass spectrum, *m/z*: 411.0300 [*M*+H]$^+$. Calcd for $C_{21}H_{13}Cl_2N_2O_3$. 411.0303.

2d: Red powder, yield 88% (0.13 g). M.p = 164.0–165.0 ^{o}C. ^{1}H-NMR ($CDCl_3$, 500 MHz): δ 8.36 (d, 1 H, *J* = 8.8 Hz, Ar-H), 7.94 (d, 1 H, *J* = 7.7 Hz, Ar-H), 7.84 (s, 1 H, CH=C), 7.68 (d, 2 H, *J* = 8.6 Hz, Ar-H), 7.45 (d, 2 H, *J* = 8.1 Hz, Ar-H), 7.30 (m, 1 H, Ar-H), 7.10 (m, 1 H, Ar-H), 6.93 (t, 1 H, *J* = 7.6 Hz, Ar-H), 6.34 (d, 1 H, Ar-H), 3.03 (s, 6 H, CH_3). ^{13}C-NMR ($CDCl_3$, 125.77 MHz): δ 167.94 (C=O), 141.44, 140.05, 136.02, 135.93 (C=C), 135.22, 132.31, 131.02, 130.52, 130.37, 128.97, 128.86, 128.46, 122.38, 122.24, 118.24, 109.00 (Ar-C), 40.36 (CH_3). Mass spectrum, *m/z*: 409.0875 [*M*+H]$^+$. Calcd for $C_{23}H_{19}Cl_2N_2O$. 409.0874.

2e: Yellow powder, yield 88% (0.13 g). Z/E molar ratio: 1:2.

^{1}H-NMR ($CDCl_3$, 500 MHz): δ 8.78 (d, 1 H, *J* = 1.7 Hz, OH), 7.86 (s, 1 H, ArH), 7.56 (d, 1 H, *J* = 7.6 Hz, ArH), 7.54 (s, 1 H, CH=C-Z isomer), 7.41 (dd, 1 H, *J* = 8.3 Hz, Ar-H), 7.33 – 7.31 (m, 2 H, Ar-H), 7.20 (m, 2 H, Ar-H), 7.19 (s, 1 H, CH=C-E isomer), 7.05 (t, 1 H, *J* = 7.5 Hz, Ar-H), 6.90 (d, 1 H, *J* = 6.5 Hz, Ar-H), 6.32 (d, 1 H, *J* = 7.7 Hz, Ar-H), 3.93 (s, 3 H, Ar-H). ^{13}C-NMR ($CDCl_3$, 125.77 MHz): δ 167.43 (C=O), 148.80, 147.55, 146.47, 139.08, 135.95, 130.70, 129.03, 126.91, 124.24, 122.78, 122.40, 114.75, 114.18, 114.07, 112.05, 109.31, 108.79, 56.13 (CH_3). Mass spectrum, *m/z*: 412.0507 [*M*+H]$^+$. Calcd for $C_{22}H_{16}Cl_2NO_3$. 412.0507.

2f: Yellow powder, yield 88% (0.13 g). M.p = 145.0–146.2 ^{o}C. ^{1}H-NMR ($CDCl_3$, 500 MHz): δ 7.87 (d, 2 H, *J* = 8.8 Hz, Ar-H), 7.52 (d, 2 H, *J* = 8.1 Hz, Ar-H), 7.38 (t, 1 H, *J* = 8.1 Hz, Ar-H), 7.28 (d, 1 H, *J* = 8.0 Hz, Ar-H), 7.25 (s, 1 H, CH=C), 7.20 (t, 1 H, *J* = 7.7 Hz, Ar-H), 7.00 (t, 1 H, *J* = 7.6 Hz, Ar-H), 6.93 (d, 1 H, *J* = 8.0 Hz), 6.41 (d, 1 H, *J* = 7.8 Hz, Ar-H), 6.07 (s, 2 H, OCHO). ^{13}C-NMR ($CDCl_3$, 125.77 MHz): δ 167.3 (C=O), 149.2, 148.0, 142.1, 138.6, 135.8, 130.7, 130.6, 129.6, 129.0 (2C), 128.7, 125.0, 124.9, 123.0, 122.5, 121.3, 109.5, 109.3, 108.7, 101.7 (OCO). Mass spectrum, *m/z*: 410.0352 [*M*+H]$^+$. Calcd for $C_{22}H_{14}Cl_2NO_3$. 410.0351.

Synthesis of 3-arylidene-1-(2,6-dichlorophenyl)-5-(methylaminosulfonyl)indolin-2-ones 5a-f

In a 50 mL reaction flask, 1-(2,6-dichlorophenyl)-5-(methylaminosulfonyl)indolin-2-one **4** (1.0 mmol) and piperazine (0.37 mmol) were dissolved in ethanol, and aldehyde (1.5 mmol) was added. The reaction mixture was refluxed for 24 h. The precipitate product was filtered and rinsed with ethanol and then with water to obtain pure product **5a-f**.

5a: Pale yellow powder, yield 65% (0.08 g). M.p = 199.0-200.3 ^{o}C. ^{1}H-NMR ($CDCl_3$, 500 MHz): δ 8.29 (s, 1 H, H^4), 8.13 (s, 1 H, CH=C), 7.76 (d, 3 H, J = 7.7 Hz), 7.59-7.51 (m, 6H), 6.55 (d, 1 H, J = 8.3 Hz), 4.33 (brd.s, 1 H, NH), 2.68 (s, 3 H, CH3). ^{13}C-NMR ($CDCl_3$, 125.77 MHz): δ 166.75 (C=O), 145.33, 141.54, 135.58, 133.91, 133.15, 131.29, 130.96, 129.77, 129.46, 129.27, 129.20, 124.70, 121.96, 121.75, 109.36, 29.43 (CH3).

Mass spectrum, *m/z*: 459.0337 $[M+H]^+$. Calcd for $C_{22}H_{17}Cl_2N_2O_3S$. 459.0337.

5b: Yellow powder, yield 83% (0.11 g). M.p = 235–236 ^{o}C. ^{1}H-NMR ($CDCl_3$, 500 MHz): δ 8.52 (d, 2 H, J = 7.4 Hz, Ar-H), 8.38 (s, 1 H, ArH), 7.96 (d, 2 H, J = 8.2 Hz), 7.95 (s, CH=C), 7.75-7.61 (dt, 5 H), 6.74 (d, 1 H), 4.77 (s, 1 H, NH), 2.93 (s, 3 H, CH_3). ^{13}C-NMR ($CDCl_3$, 125.77 MHz): δ 164.50 (C=O), 143.53, 139.84, 137.91, 135.58, 134.02 (2C), 133.10 (Ar-C), 131.60, 131.30 (C=C), 129.76, 129.13 (2C), 128.86 (2C), 128.54, 125.08, 123.54, 118.84, 109.21 (Ar-C) 29.50 (CH_3). Mass spectrum, *m/z*: 492.9917 $[M+H]^+$. Calcd for $C_{22}H_{16}Cl_3N_2O_3S$. 492.9947.

5c: Pale yellow powder, yield 65% (0.09 g). Z/E molar ratio: 1:1.

^{1}H-NMR ($CDCl_3$, 500 MHz): δ 9.16 (s, 1 H, $H^{2'}$–Z isomer), 8.68 (s, 1 H, $H^{2'}$ -E isomer), 8.60 (d, 1 H, J = 7.9 Hz, $H^{6'}$), 8.33-8.31 (dd, H^4), 8.16 (dd, J = 9.9 Hz, H^7), 8.0 (s, 1 H, CH=C- Z isomer), 7.97 (d, 1 H, J = 7.7 Hz, Ar-H), 7.80 (s, 1 H, CH=C Z isomer), 7.76-7.73 (m, 1 H, Ar-H), 7.62 (t, 1 H, J = 8.1 Hz, Ar-H), 6.54 (dd, 2 H, J = 8.3 Hz, Ar-H), 4.36-4.33 (m, 1 H, NH), 2.73 (d, 3 H, J = 5.3 Hz, CH_3 Z isomer), 2.69 (d, CH_3, J = 5.3 Hz, E isomer).^{13}C-NMR ($CDCl_3$, 125.77 MHz): δ 164.65, 147.90, 137.22, 136.78, 135.27, 135.12, 133.18, 131.08, 130.16, 130.09, 129.06, 128.85, 128.78, 126.44, 124.66, 123.22, 121.69, 118.93, 109.32, 33.06. Mass spectrum, *m/z*: 504.0188 $[M+H]^+$. Calcd for $C_{22}H_{16}Cl_3N_2O_3S$. 504.0188.

5d: Red powder, yield 74% (0.1 g). ^{1}H-NMR ($CDCl_3$, 500 MHz): δ 8.47 (d, 2 H, J = 9.0 Hz, Ar-H), 8.1 (m, 1 H, Ar-H), 7.7 (s, 1 H, C*H*=C), 7.65-7.64 (dd, 1 H, J = 8.2, Ar-H), 7.54 (d, 2 H, J = 8.1 Hz, Ar-H), 7.40 (t, 1 H, J = 8.0 Hz, Ar-H), 6.71 (d, 2 H, J = 9.1 Hz, Ar-H), 6.51 (d, 1 H, J = 8.2 Hz, Ar-H), 4.32 (d, 1 H, J = 5.5 Hz, NH), 3.10 (s, 6 H, NC*H*), 2.72 (d, 3 H, J = 5.4 Hz, CH_3). ^{13}C-NMR ($CDCl_3$, 125.77 MHz): δ 165.19 (C=O), 152.87, 142.33, 142.04, 136.10, 135.82, 132.08, 130.86, 129.00, 126.80, 126.10, 121.99, 117.24,

116.21, 111.28, 108.51, 103.69, 40.04 (2C, CH_3), 29.57 (CH_3). Mass spectrum, *m/z*: 502.0760 $[M+H]^+$. Calcd for $C_{24}H_{22}Cl_2N_3O_3S$. 502.0759.

5e: Red power, yield 85% (0.14 g). Z/E molar ratio: 1:2

^{1}H-NMR (DMSO-d_6, 500 MHz): δ 8.61 (s, 1 H, OH), 8.41 (s, 1 H, ArH-Z isomer), 7.93 (s, 2 H, ArH-E isomer), 7.76 (d, 2 H, J = 8.2 Hz, ArH–E isomer), 7.62 (d, 1 H, J = 8.2 Hz, ArH–Z isomer), 7.58 (s,1 H, C=CH-Z isomer), 7.55 (s, 2 H, C=CH-E isomer), 7.44 (d, 1 H, J = 8.1 Hz, ArH), 7.22 (m, 1 H, ArH), 6.53 (d, 1 H, J = 8.2 Hz, ArH), 6.26 (d, 1 H, J = 8.2 Hz, ArH), 3.76 (s, 3 H, CH_3-Z isomer), 3.65 (s, 3 H, CH_3-E isomer), 2.46 (s, 6 H, CH_3-E isomer), 2.40 (s, 6 H, CH_3-Z isomer). ^{13}C-NMR (DMSO-d_6, 125.77 MHz): δ 168.00, 164.81, 150.99, 142.73, 141.31, 138.55, 135.56, 135.39, 132.05, 131.86, 129.71, 129.64, 129.16, 121.71, 120.59, 117.34, 114.30, 107.85, 107.10, 55.06, 29.43. Mass spectrum, *m/z*: 505.0390 $[M+H]^+$. Calcd for $C_{23}H_{19}Cl_2N_2O_5S$. 505.0392.

5f: Yellow powder, yield 81% (0.11 g). Z/E molar ratio 1:1.3.

^{1}H-NMR ($CDCl_3$, 500 MHz): δ 8.48 (d, 1 H, J = 1.5 Hz, H^4), 8.40 (s, 1 H, H^4), 8.12 (s, 1 H, CH=C), 7.98 (s, 1 H, CH=C), 7.69 – 7.67 (dd, 1 H, J = 8.3 Hz, ArH), 7.56 (s, 1 H, ArH), 7.45 (d, 1 H, ArH), 7.42 – 7.41 (m, 1 H, ArH), 7.34 (s, 1 H, ArH), 7.24 (s, 1 H, ArH), 6.91 (d, 1 H, J = 8.2 Hz, ArH), 6.54 (m, 1 H, ArH), 6.05 (s, 2 H, CH_2), 4.39 (s, 1 H, NH), 2.73 (s, 3 H), 2.71 (s, 3 H). ^{13}C-NMR ($CDCl_3$, 125.77 MHz): δ 167.01, 150.13, 148.38, 148.10, 145.12, 141.50, 135.61, 131.23, 130.69, 129.17, 128.87, 127.66, 125.53, 122.98, 121.80, 120.60, 111.98, 109.39, 108.99, 108.38, 101.96, 29.50. Mass spectrum, *m/z*: 503.0237 $[M+H]^+$. Calcd for $C_{23}H_{17}Cl_2N_2O_5S$. 503.0235.

3. NMR Spectra

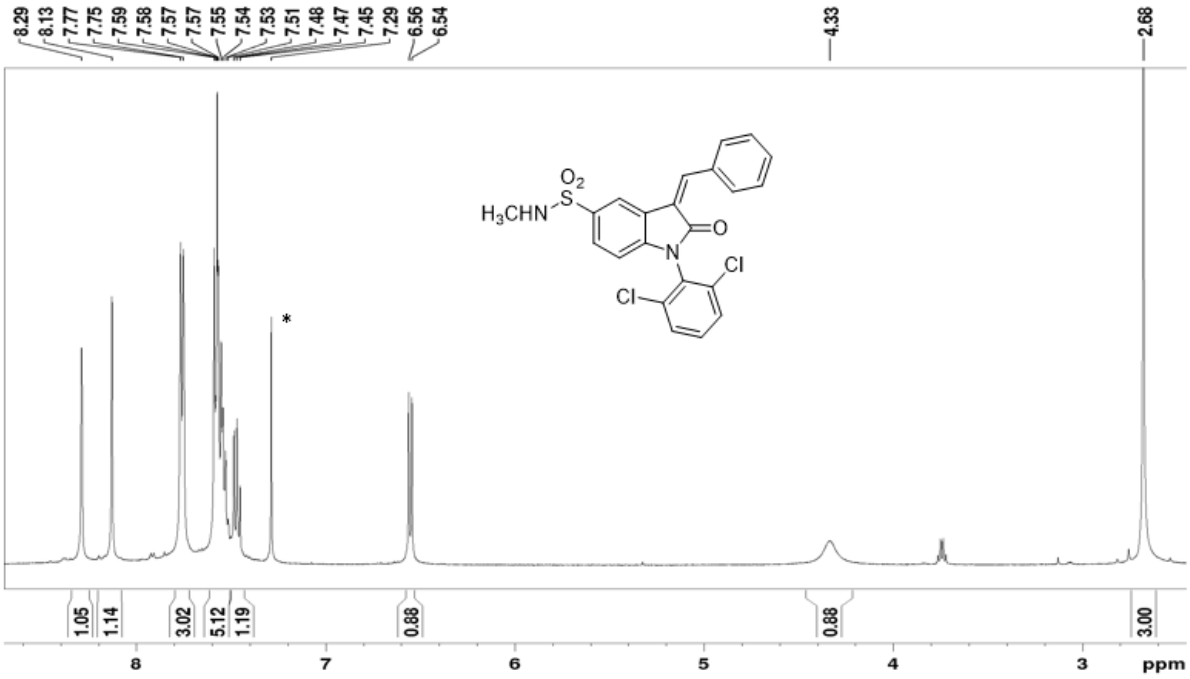

Figure S1: ^{1}H NMR spectrum of **5a** in $CDCl_3$ (500MHz, *-$CDCl_3$ solvent residual signal)

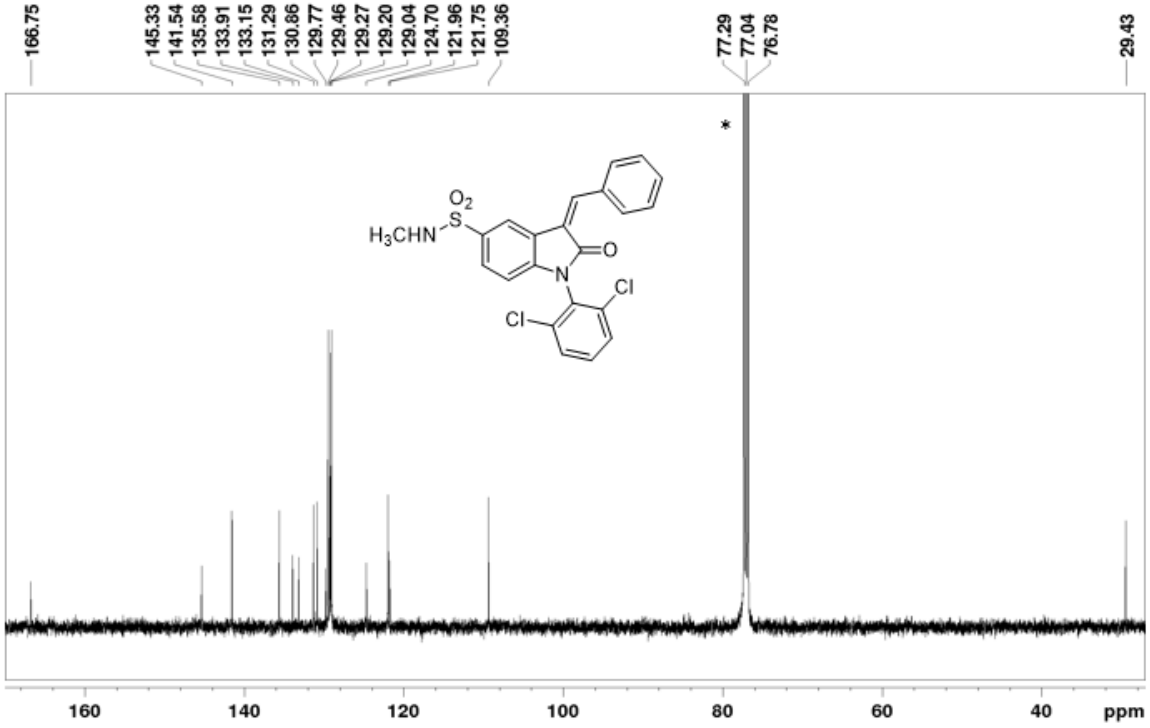

Figure S2: ^{13}C {^{1}H} NMR spectrum of **5a** in $CDCl_3$ (125MHz, *-$CDCl_3$ solvent residual signal)

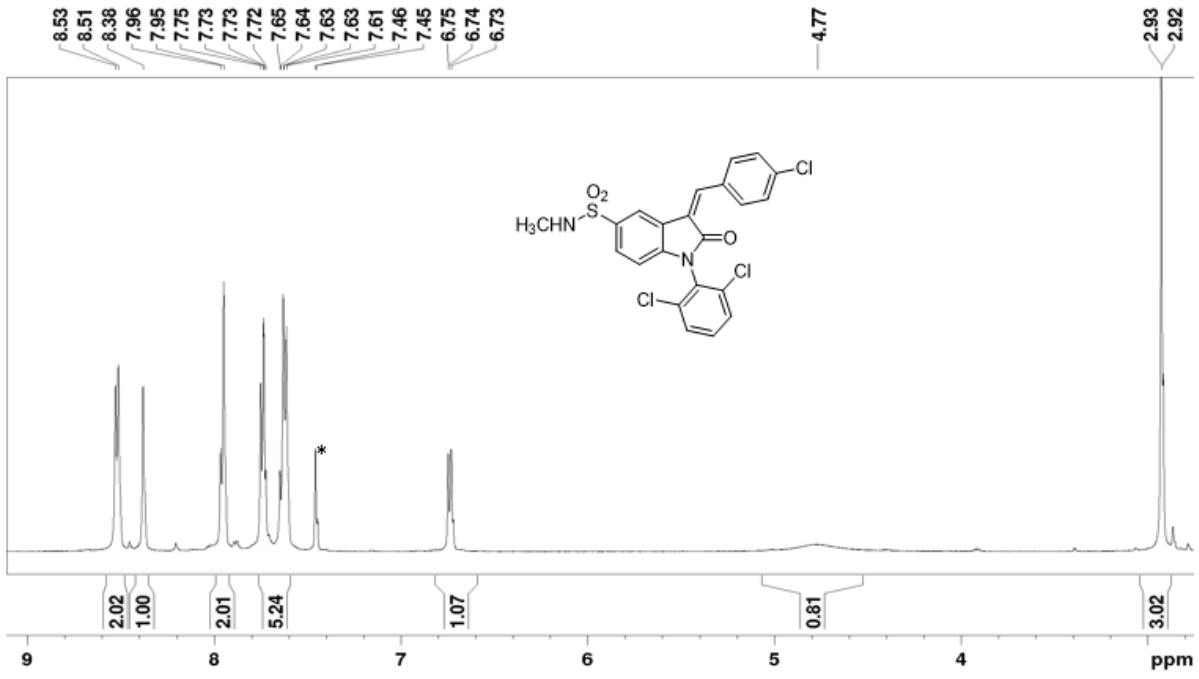

Figure S3: ^{1}HNMR spectrum of **5b** in $CDCl_3$ (500MHz, *-$CDCl_3$ solvent residual signal)

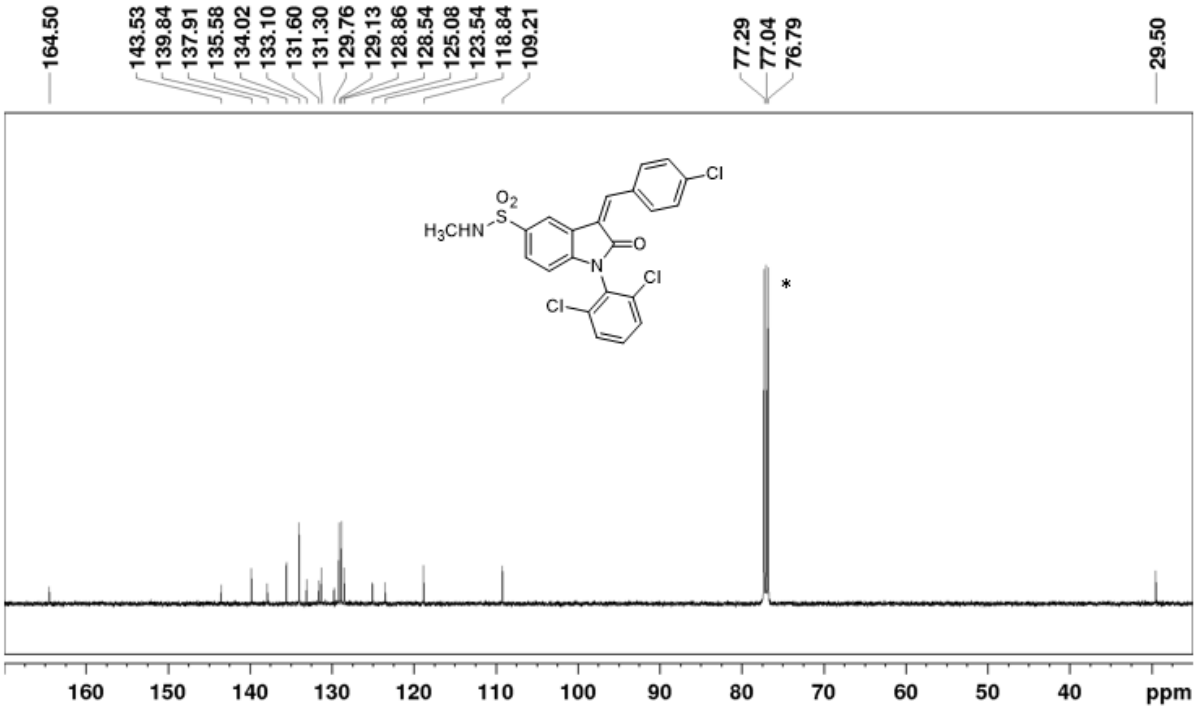

Figure S4: ^{13}C {^{1}H} NMR spectrum of **5b** in $CDCl_3$ (125MHz, *-$CDCl_3$ solvent residual signal)

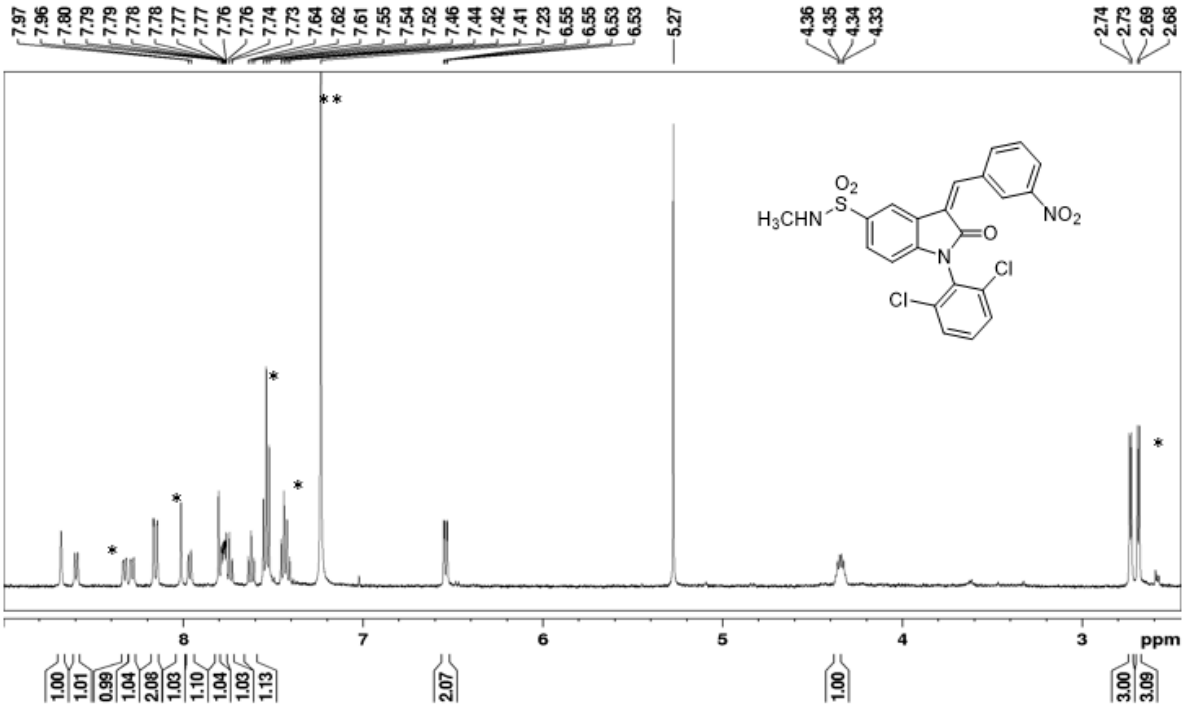

Figure S5: ^{1}HNMR spectrum of **5c** in $CDCl_3$ (500MHz, **-$CDCl_3$ solvent residual signal, *-Z isomer)

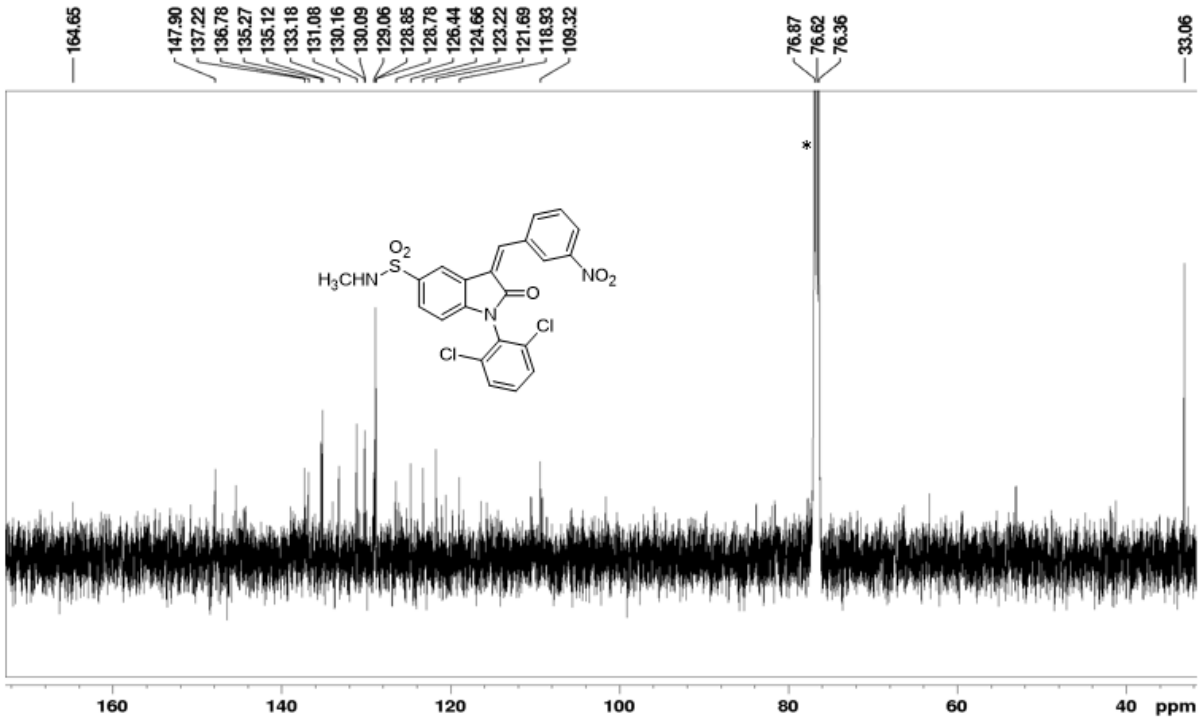

Figure S6: ^{13}C {^{1}H} NMR spectrum of **5c** in $CDCl_3$ (125MHz, *-$CDCl_3$ solvent residual signal)

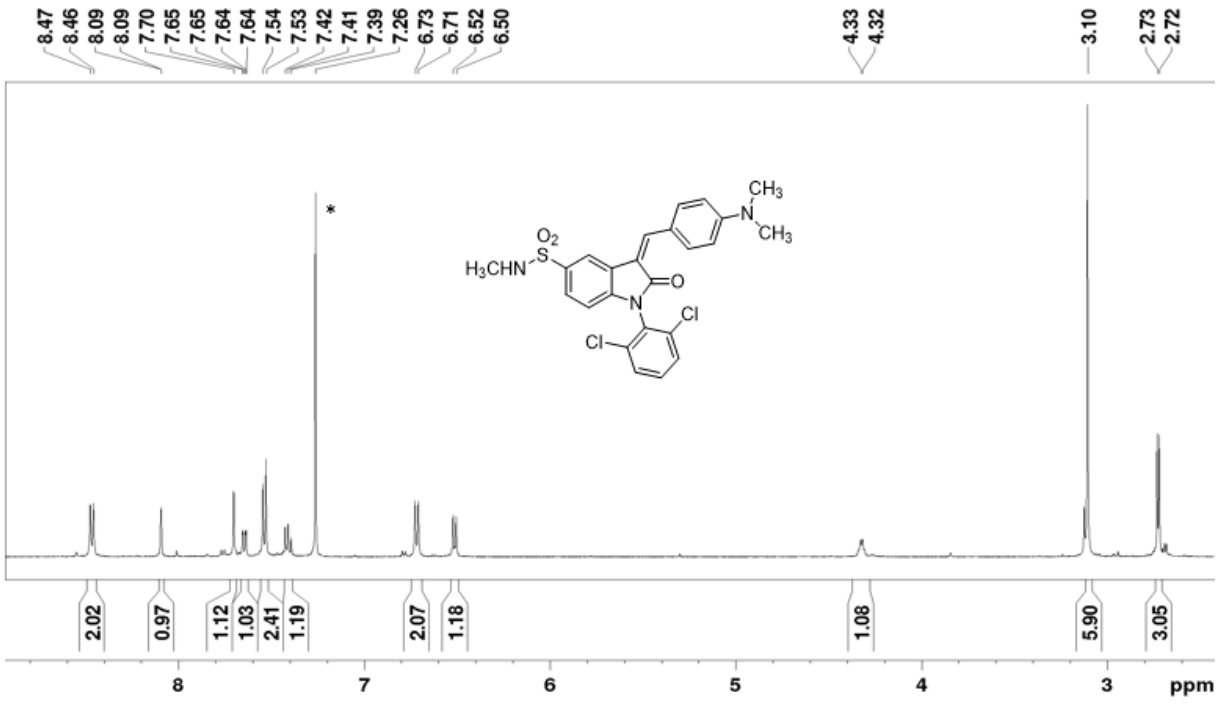

Figure S7: ^{1}HNMR spectrum of **5d** in $CDCl_3$ (500MHz, *-$CDCl_3$ solvent residual signal)

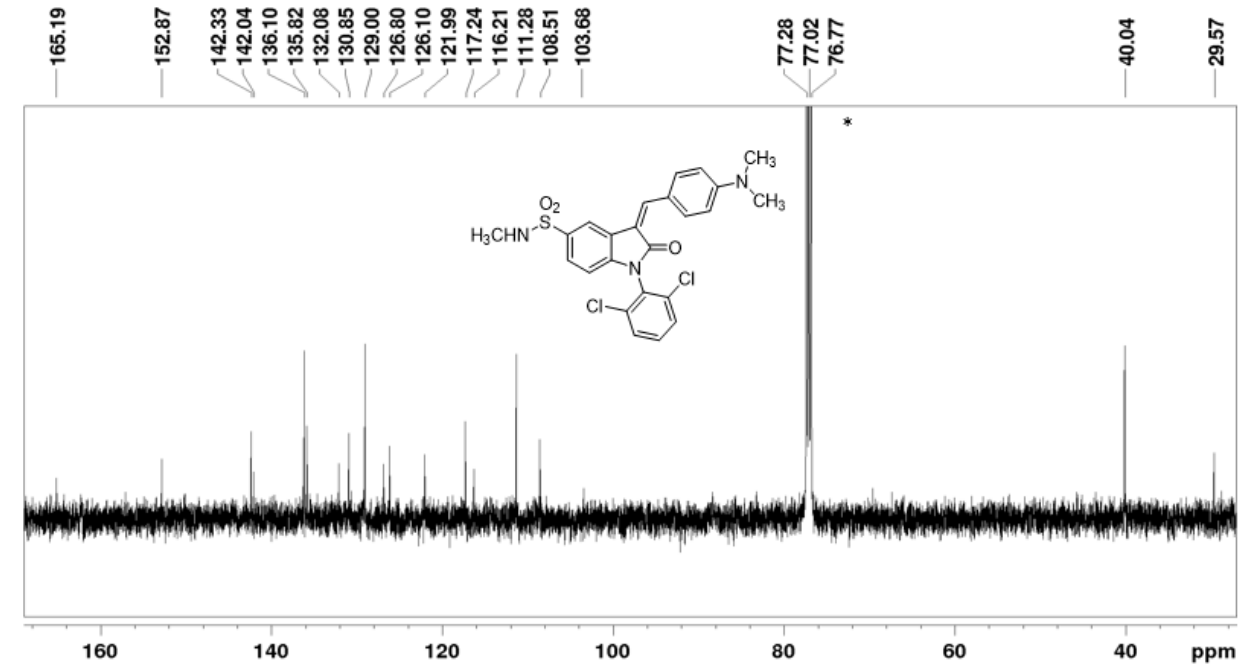

Figure S8: ^{13}C {^{1}H} NMR spectrum of **5d** in $CDCl_3$ (125MHz, *-$CDCl_3$ solvent residual signal)

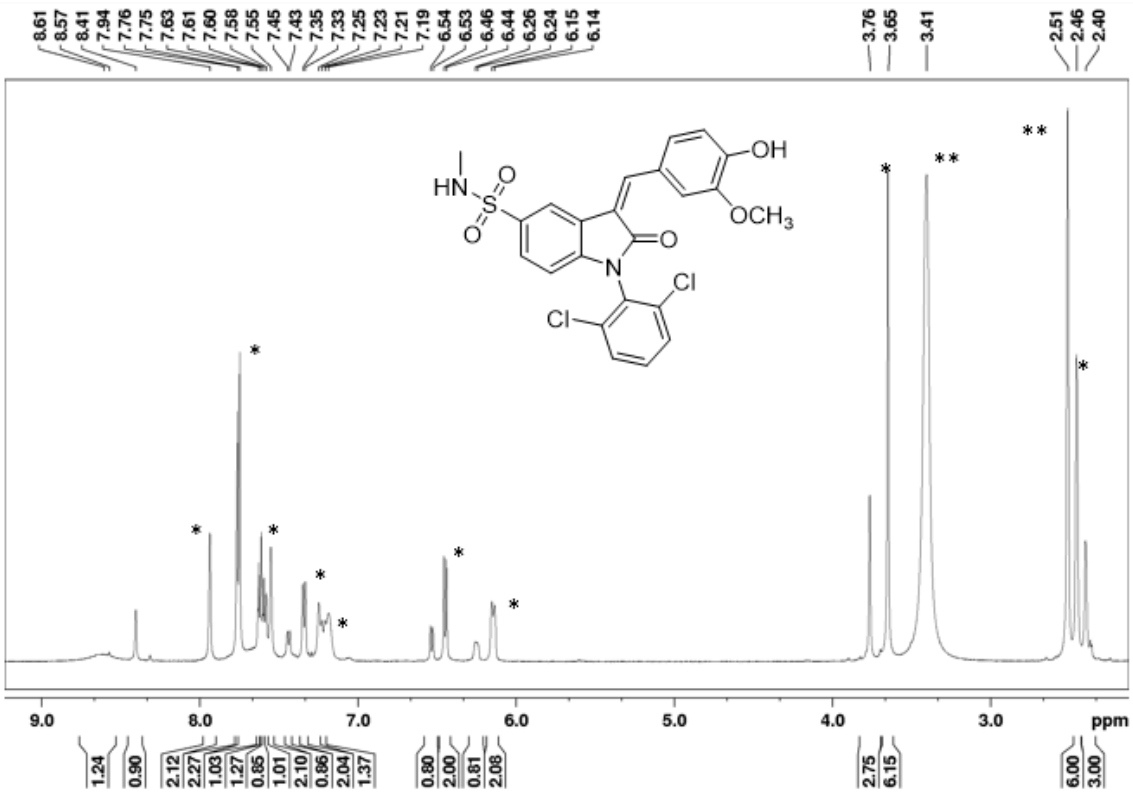

Figure S9: ^{1}HNMR spectrum of **5e** in DMSO-d_6 (500MHz, **- DMSO solvent residual signal, *- Z isomer)

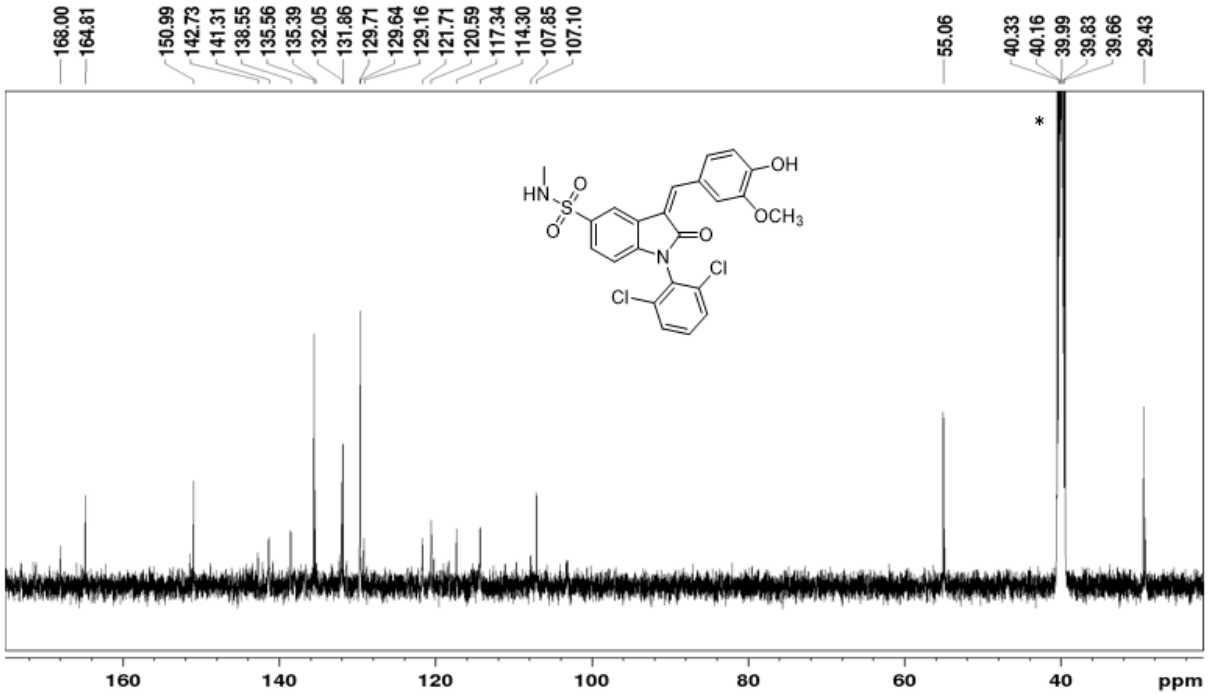

Figure S10: ^{13}C {^{1}H} NMR spectrum of **5e** in DMSO-d_6 (125MHz, *- solvent residual signal)

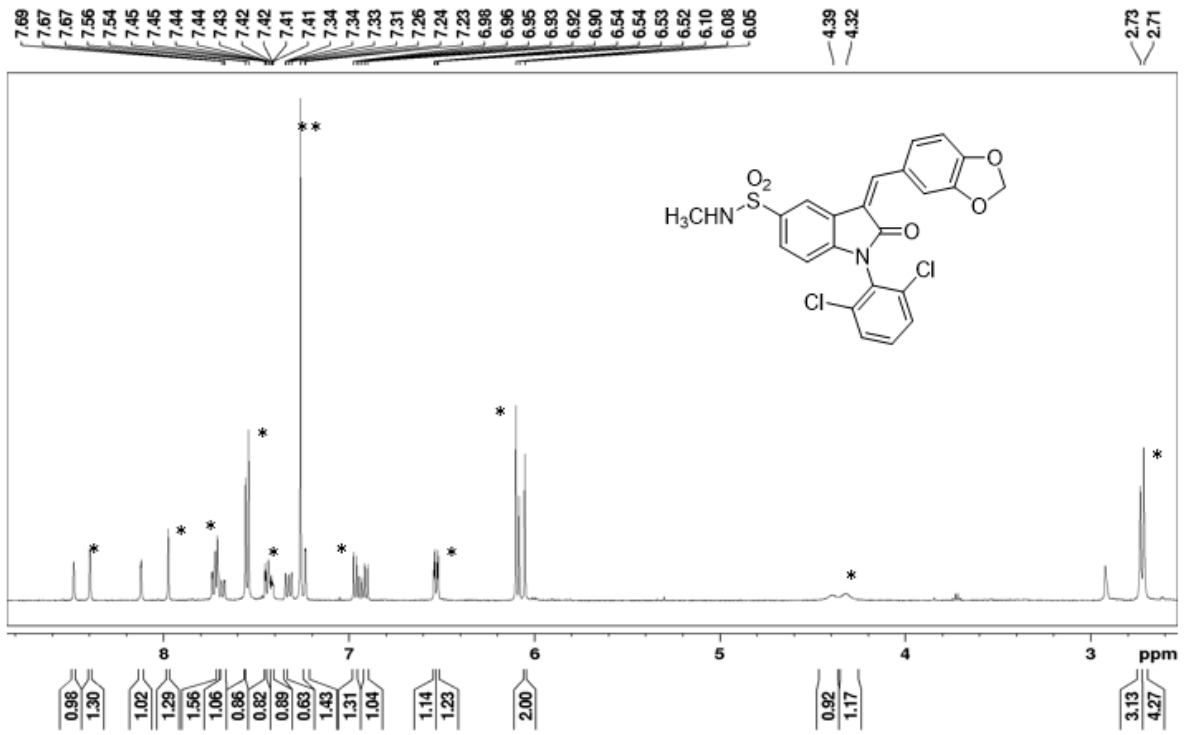

Figure S11: ^{1}H NMR spectrum of **5f** in $CDCl_3$ (500MHz, **- $CDCl_3$ solvent residual signal, *- Z isomer)

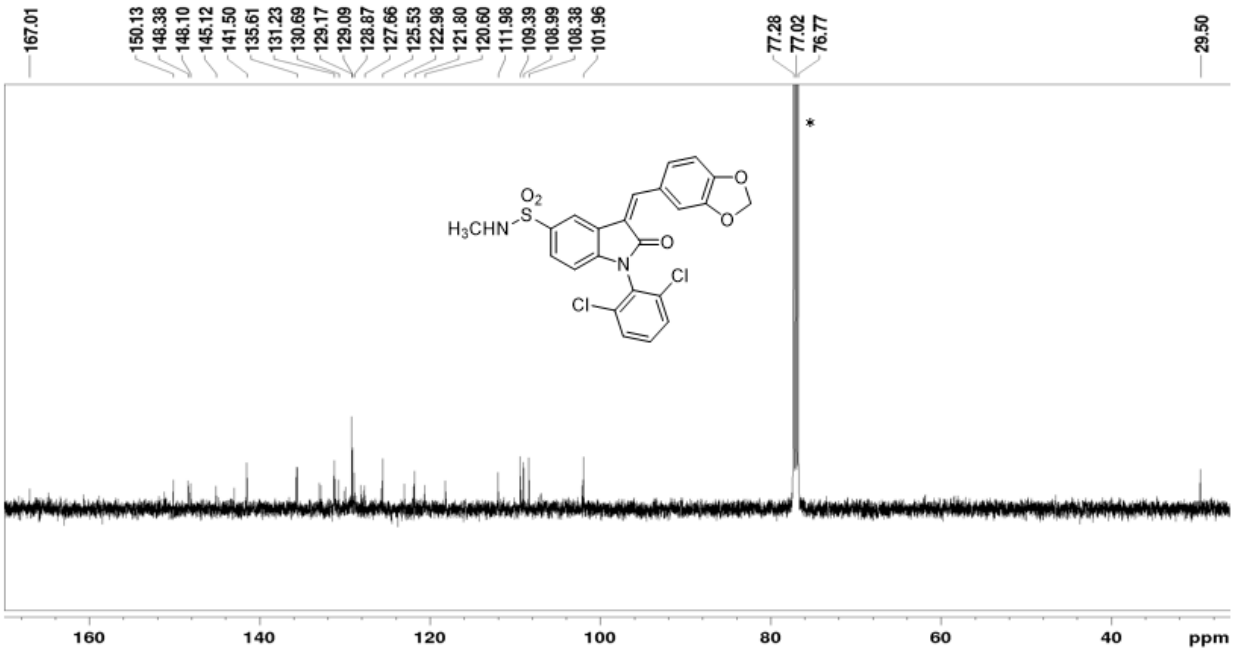

Figure S12: ^{13}C {^{1}H} NMR spectrum of **5f** in $CDCl_3$ (125MHz, *-$CDCl_3$ solvent residual signal)

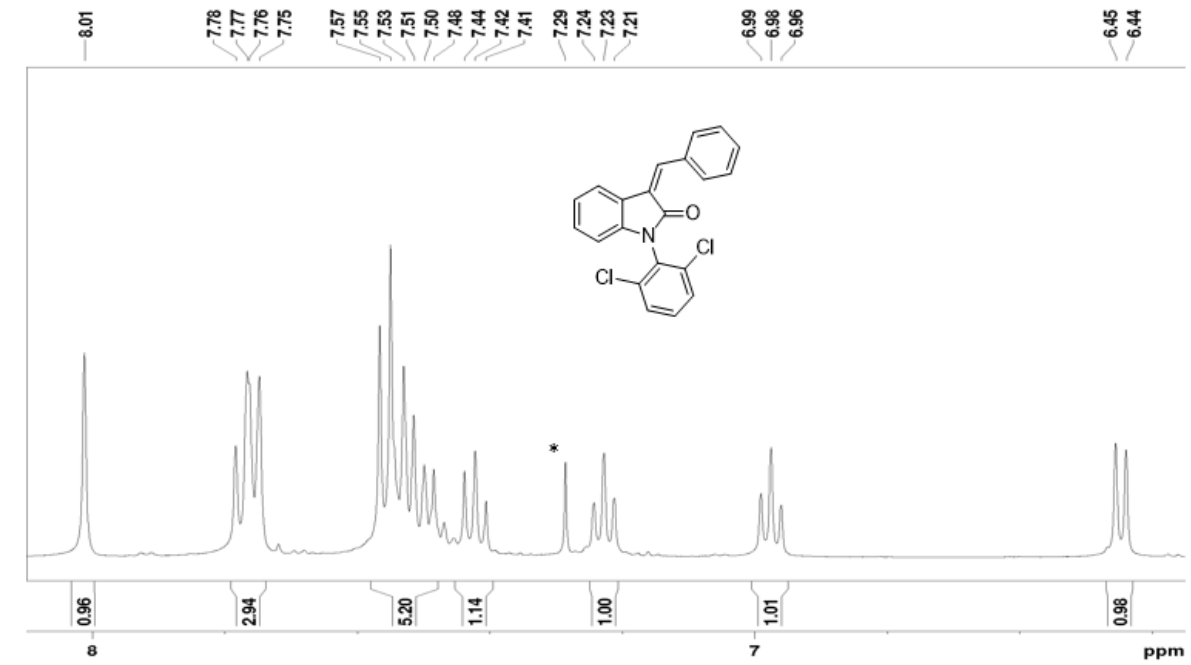

Figure S13: ^{1}H NMR spectrum of **2a** in $CDCl_3$ (500MHz, *-$CDCl_3$ solvent residual signal)

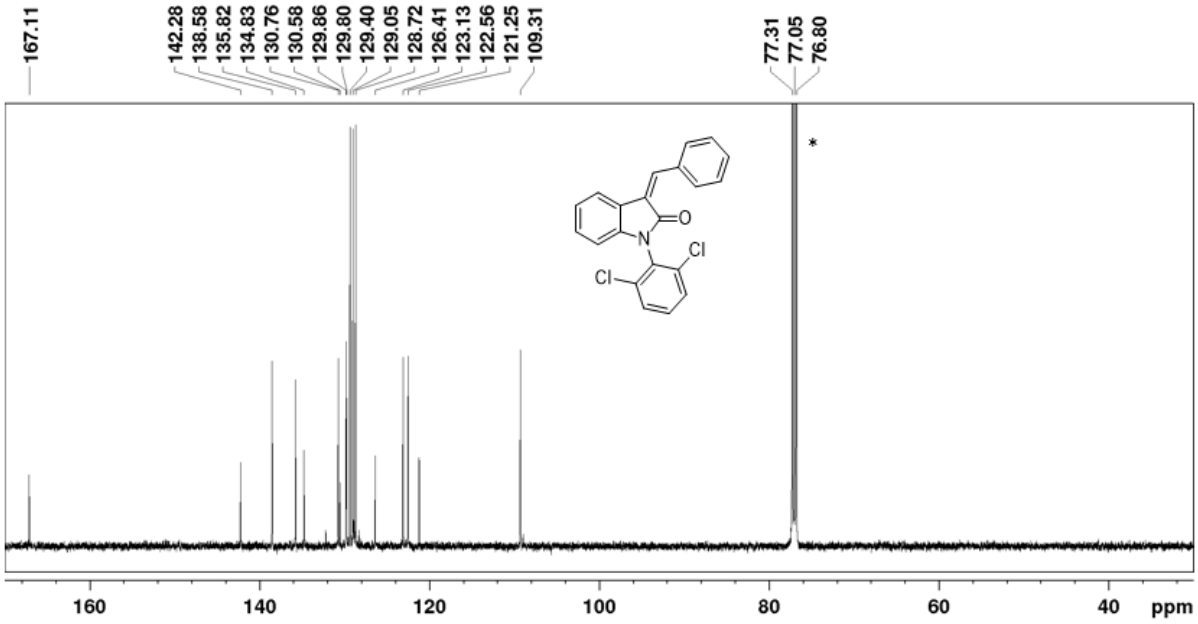

Figure S14: ^{13}C {^{1}H} NMR spectrum of **2a** in $CDCl_3$ (125MHz, *-$CDCl_3$ solvent residual signal)

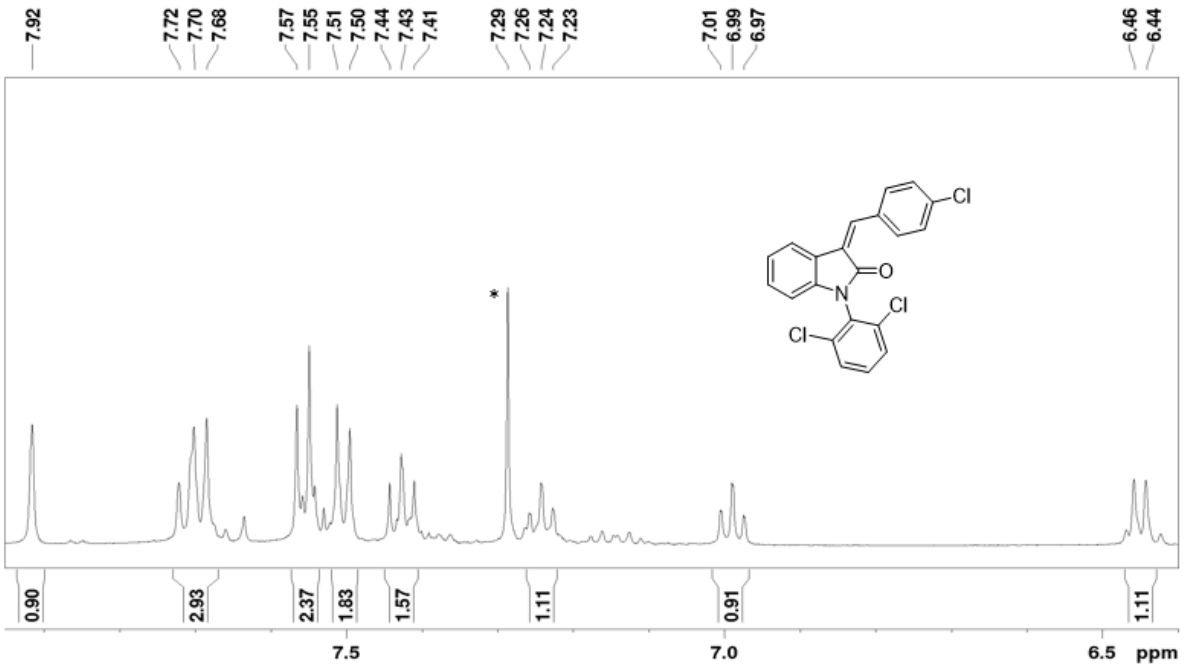

Figure S15: ^{1}H NMR spectrum of **2b** in $CDCl_3$ (500MHz, *-$CDCl_3$ solvent residual signal)

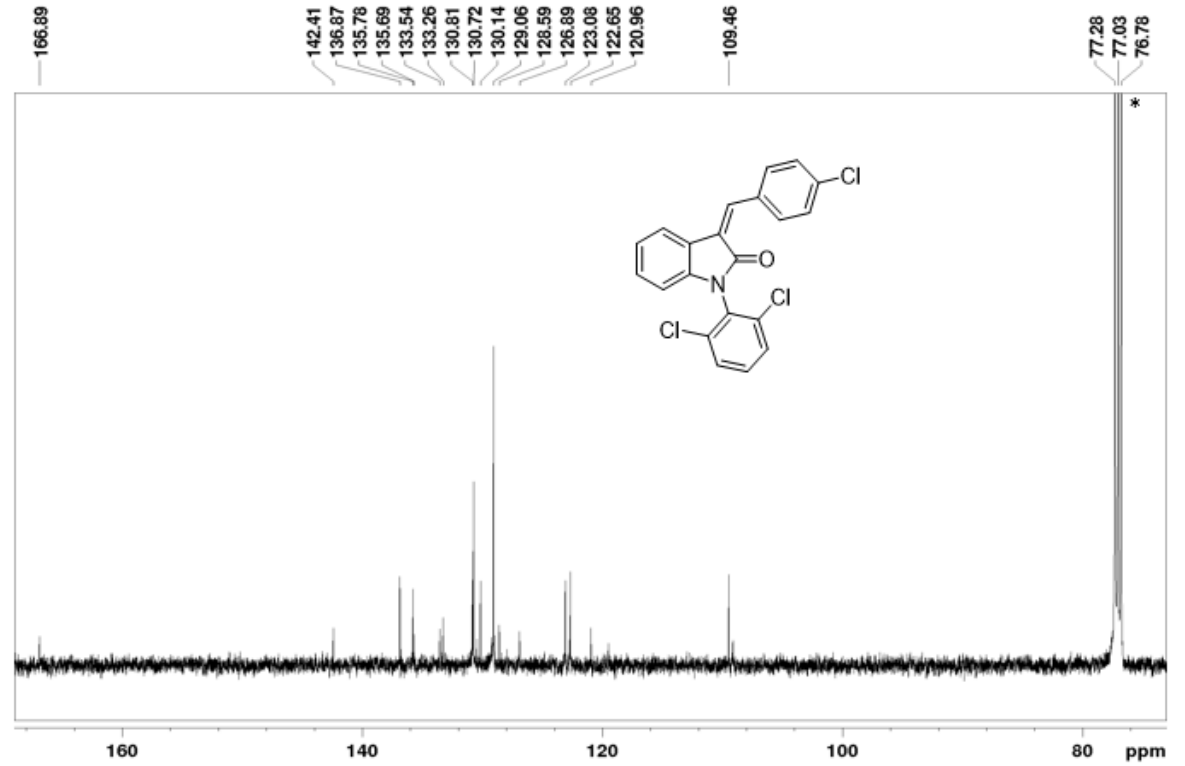

Figure S16: ^{13}C {^{1}H} NMR spectrum of **2b** in $CDCl_3$ (125MHz, *-$CDCl_3$ solvent residual signal)

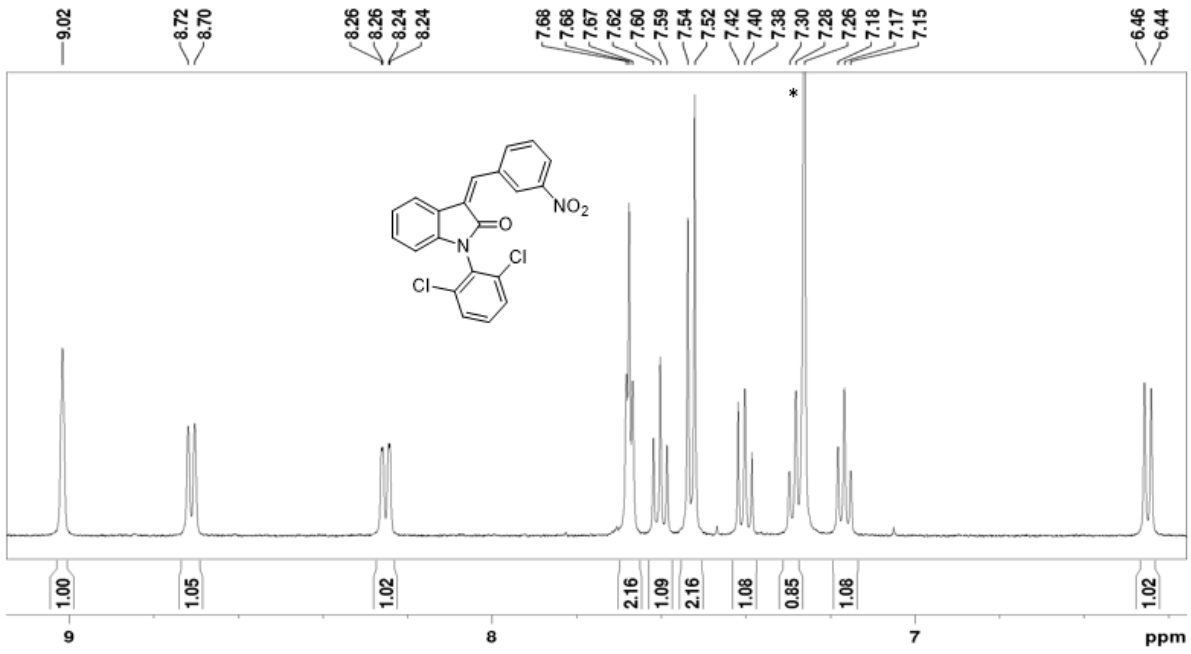

Figure S17: ^{1}H NMR spectrum of **2c** in $CDCl_3$ (500MHz, *-$CDCl_3$ solvent residual signal)

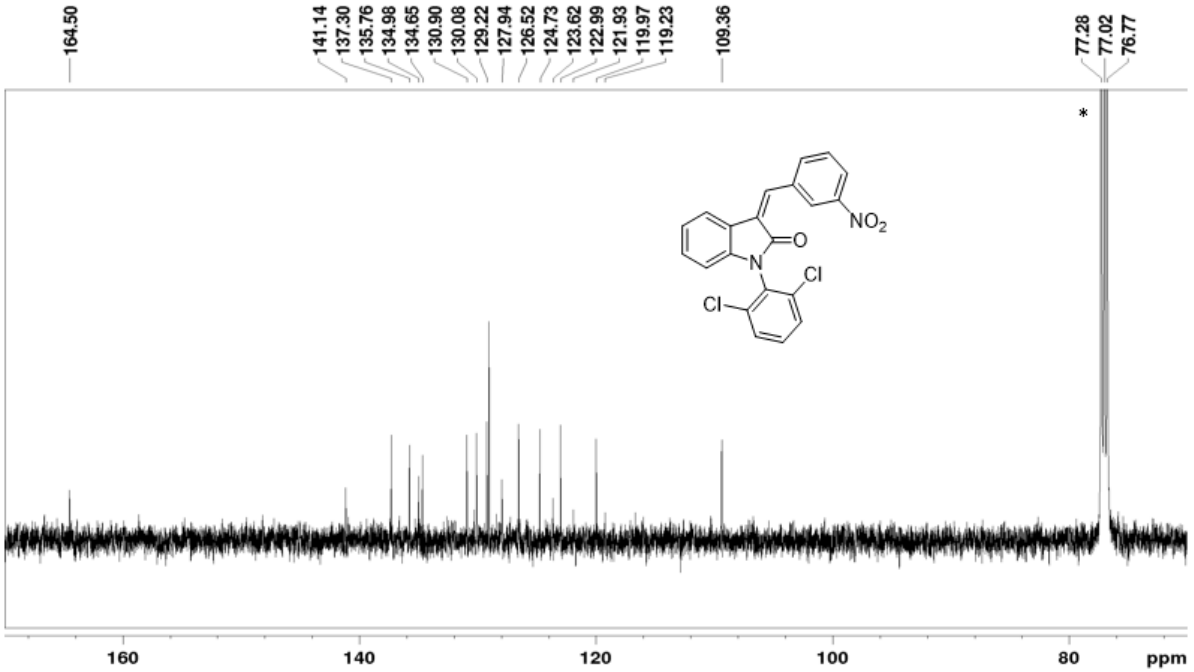

Figure S18: ^{13}C {^{1}H} NMR spectrum of **2c** in $CDCl_3$ (125MHz, *-$CDCl_3$ solvent residual signal)

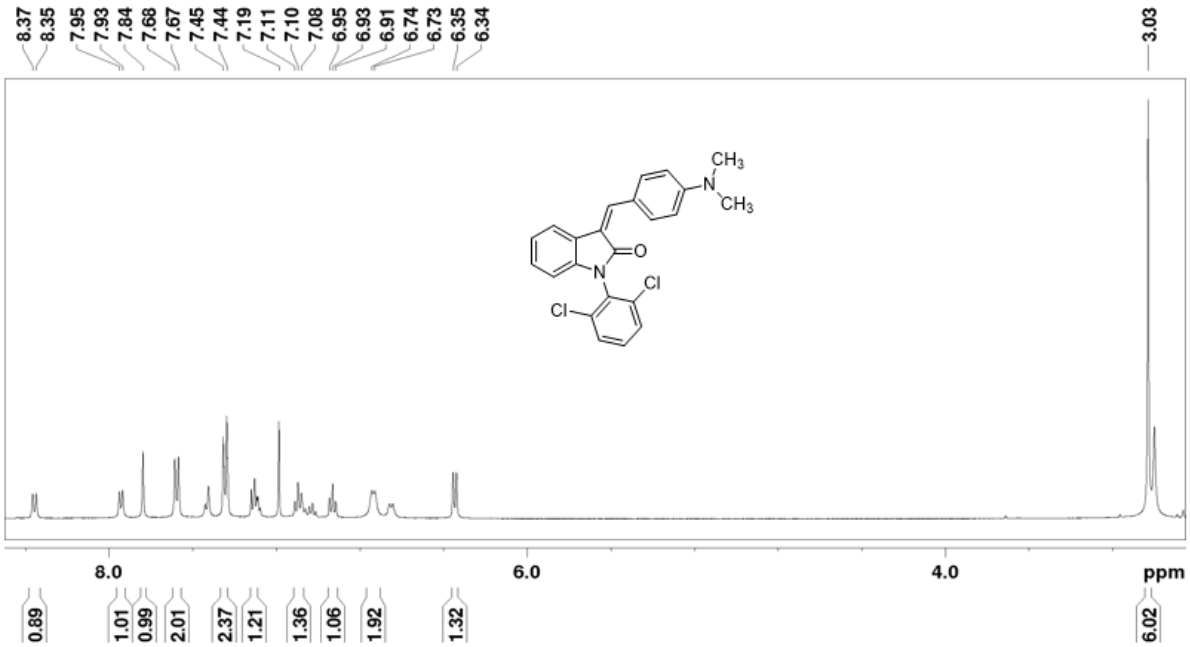

Figure S19: ^{1}H NMR spectrum of **2d** in $CDCl_3$ (500MHz, *-$CDCl_3$ solvent residual signal)

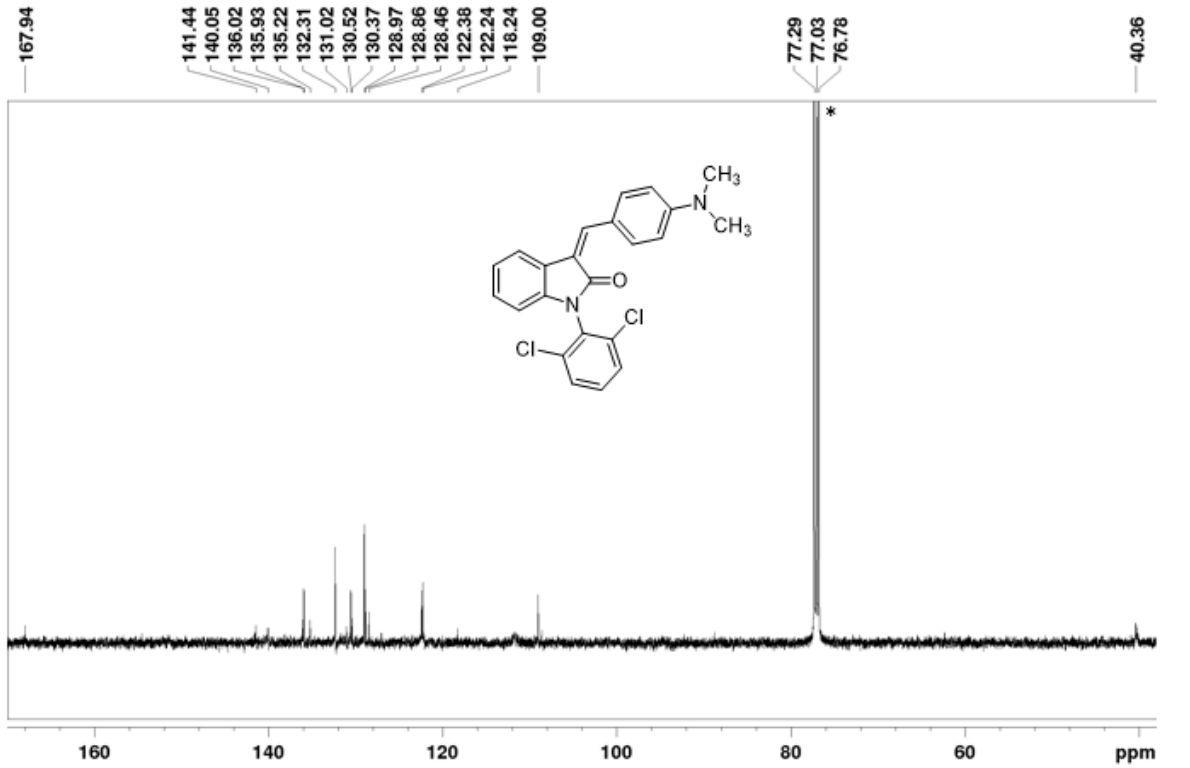

Figure S20: ^{13}C {^{1}H} NMR spectrum of **2d** in $CDCl_3$ (125MHz, *-$CDCl_3$ solvent residual signal)

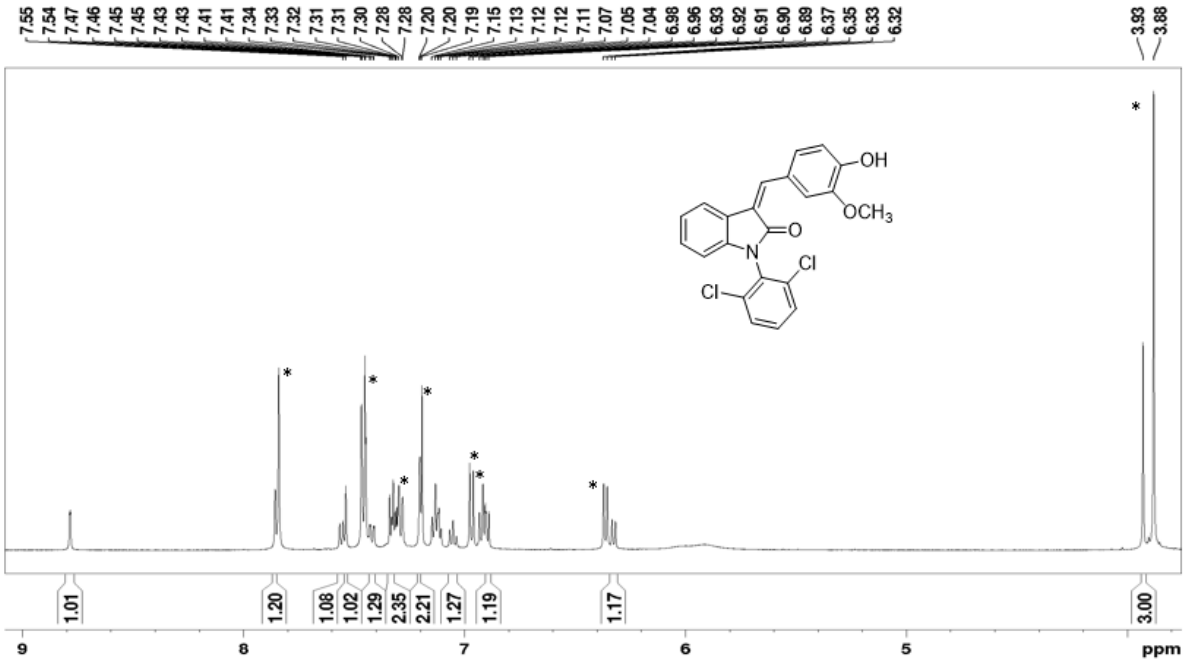

Figure S21: ^{1}H NMR spectrum of **2e** in $CDCl_3$ (500MHz, *-other isomer)

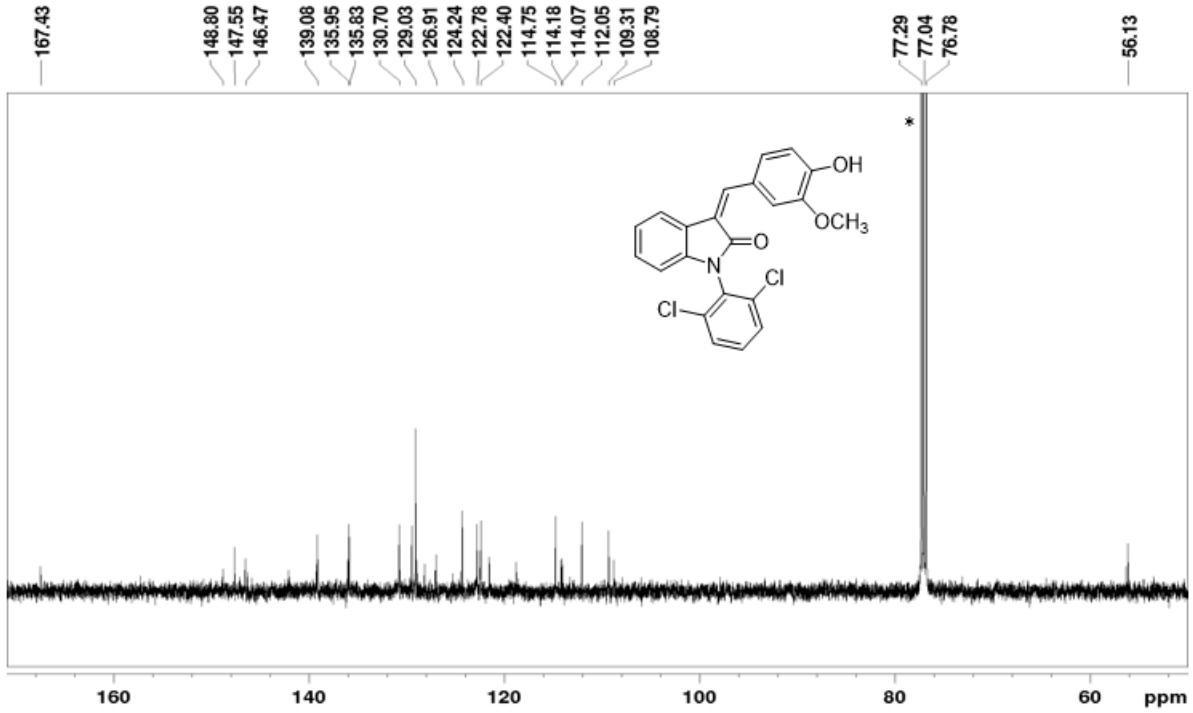

Figure S22: ^{13}C {^{1}H} NMR spectrum of **2e** in $CDCl_3$ (125MHz, *-$CDCl_3$ solvent residual signal)

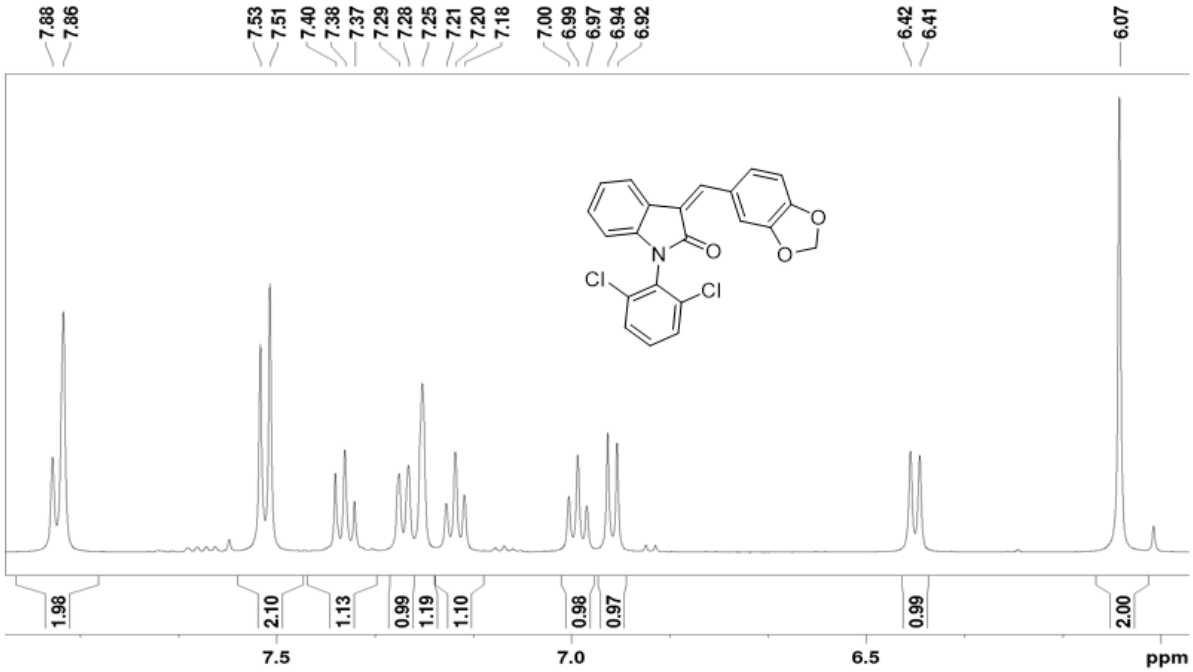

Figure S23: ^{1}HNMR spectrum of **2f** in $CDCl_3$ (500MHz, *-$CDCl_3$ solvent residual signal)

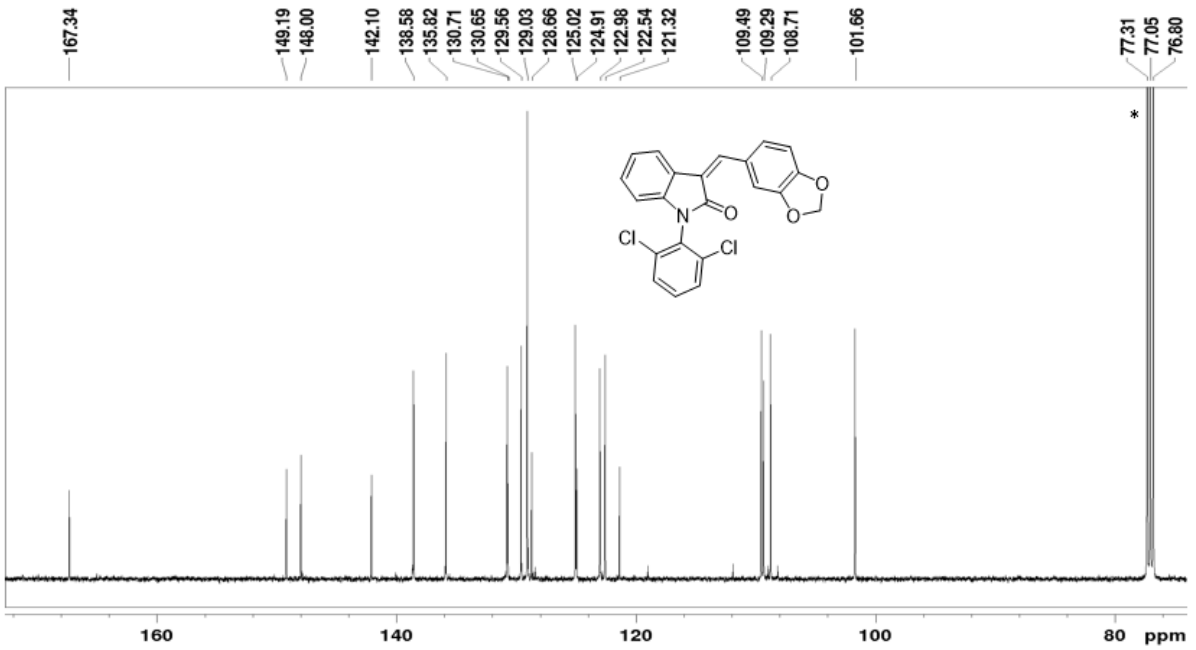

Figure S24: ^{13}C {^{1}H} NMR spectrum of **2f** in $CDCl_3$ (125MHz, *-$CDCl_3$ solvent residual signal)

4. α-Glucosidase inhibition assay

The α-glucosidase inhibition assay had been carried out on 96-well plate according to previously reported work.[S1] The test compounds were dissolved in DMSO to prepare 1024, 256, 64, 16, 4, 1 μg mL^{-1} concentrations. To each well plate, were added 40 μL phosphate buffer 100 mM pH 6.8, 25 μL α-glucosidase (EC 3.2.1.20) 0.4 U/mL and 10 μL test compound. The mixture was incubated at 37 °C for 15 min then 25 μL *p*-nitrophenyl α-D-glucopyranoside 2.5 mM was added followed by incubation at 37 °C for 30 min. Na_2CO_3 was added to stop the reaction and the absorbance was measured spectrophotometrically at 410 nm. In the negative control, the test solution was replaced by DMSO. Acarbose was used as a positive control. All experiments were carried out in triplicates. The % inhibition was calculated using the equation: Inhibition (%) = $1-\frac{A_{sample}}{A_{control}}$ *100%. IC_{50} value is defined as a concentration of test compound inhibiting 50% of α-glucosidase activity.

5. Molecular docking

Docking studies were carried using AutoDock Vina. The structure of *α*-glucosidase enzyme was obtained from protein database (PDB ID 3A4A).[S2] The Ca^{2+} cation and small molecules in the protein structures were removed and the protein structure was prepared using Autodock Tool. The structures of the indolones were optimized using Gaussian 16 prior to docking. The docking were perform with exhaustiveness of 100 and cut off energy thread hood was set to be 6 kcal/mol. Analysis were based on the 9 complexes with highest interaction energy.

Binding of the indolones with the protein are spotted at the active site of the protein (Figure S25). A comparison of binding energy and binding pattern for the complexes with highest interaction energy of sulfonamide-free (*Z*-**2b**, *Z*-**2c**, *Z*-**2f**) and the sulfonamide (*Z*-**5c**, *Z*-**5e**Z, *Z*-**5f**) are presented in Tables S1-S6. In all cases, there are two conformations with highest binding energies and all the other are significantly lower. However, close examinations reveal that for each complexes, the difference between the two most stable conformations are minimal and the ligands share the same binding pattern (interactions and amino acids involved). Therefore, selection of the most stable conformations for analysis was made by software default.

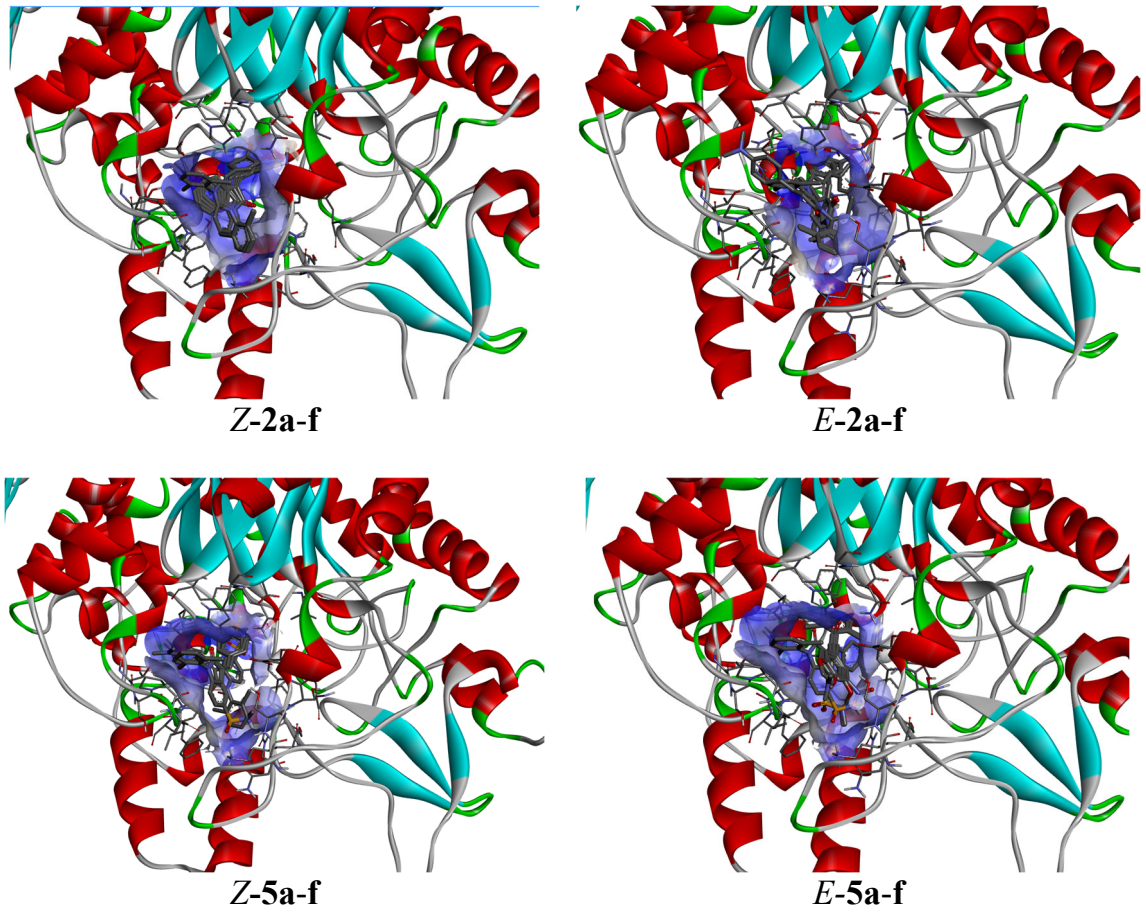

Figure S25. Alignment of the indolones in the α-glucosidase enzyme binding pocket.

Table S1 Comparison of binding mode and binding energy of the most favourable *Z*-**2b**-3A4A complex.

Mode	Affinity (kcal mol^{-1})	Binding mode	
1	-10.0	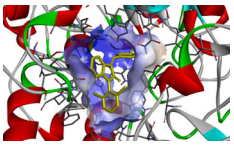	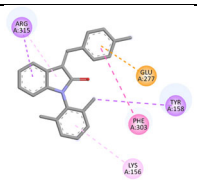
2	-10.0	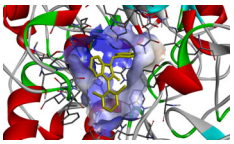	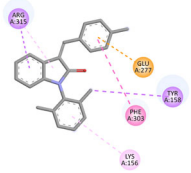
3	-9.7	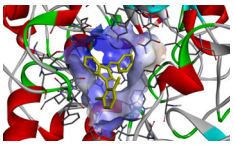	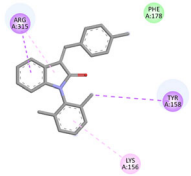
4	-9.6	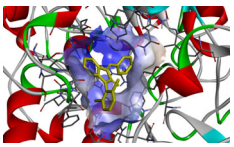	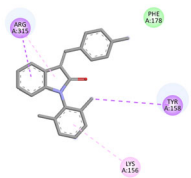
5	-9.5	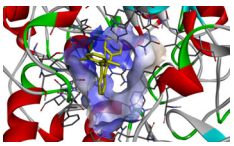	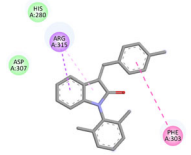
6	-9.4	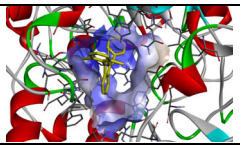	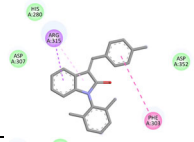
7	-9.4	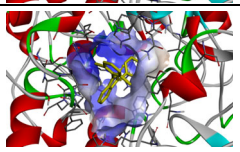	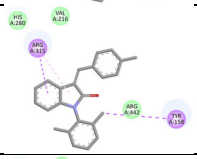
8	-9.4	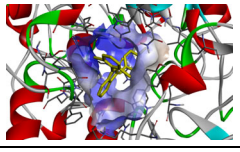	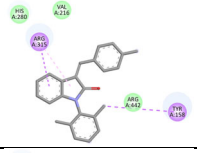
9	-9.3	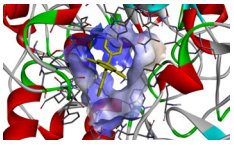	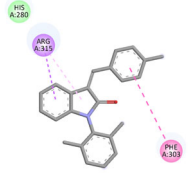

Table S2. Comparision of binding mode and binding energy of the most favourable *Z*-**2c**-3A4A complex.

Mode	Affinity (kcal mol^{-1})	Binding mode	
1	-10.5	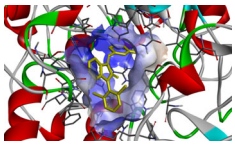	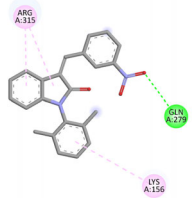
2	-10.5	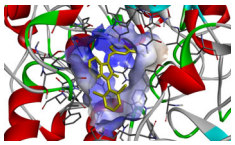	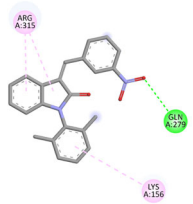
3	-10.2	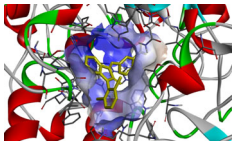	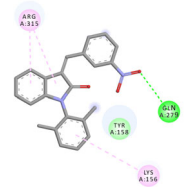
4	-9.9	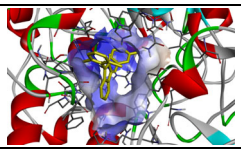	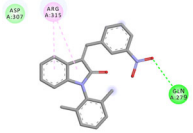
5	-9.8	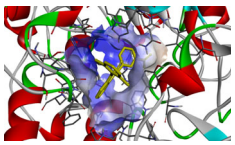	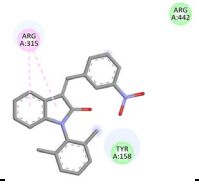
6	-9.7	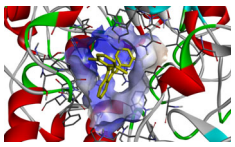	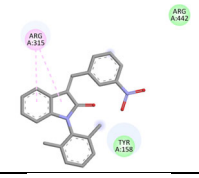
7	-9.6	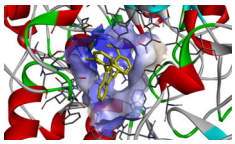	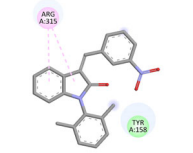
8	-9.4	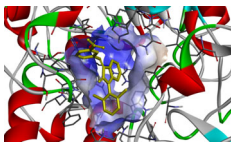	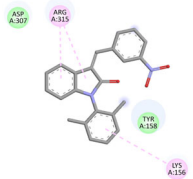
9	-9.4	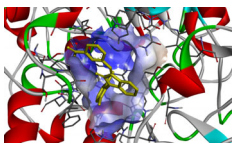	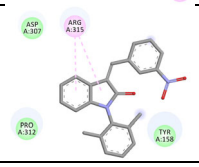

Table S3. Comparision of binding mode and binding energy of the most favourable *Z*-**2f**-3A4A complex.

Mode	Affinity (kcal mol^{-1})	Binding mode	
1	-10.8	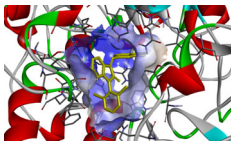	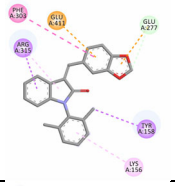
2	-10.7	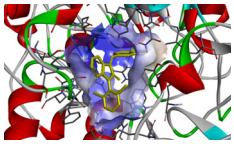	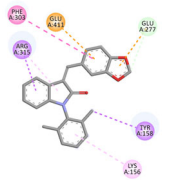
3	-10.3	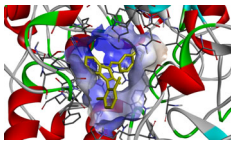	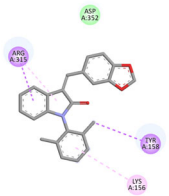
4	-10.3	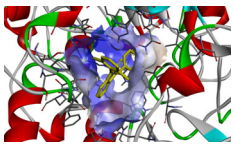	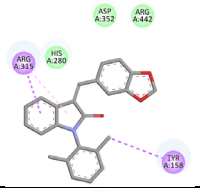
5	-10.3	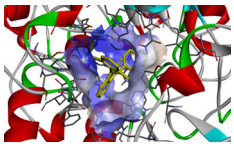	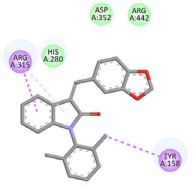
6	-9.9	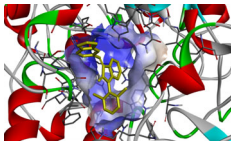	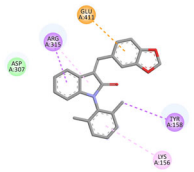
7	-9.9	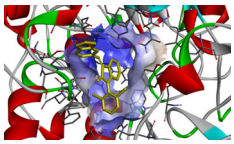	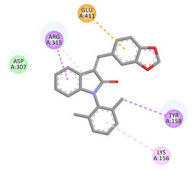
8	-9.8	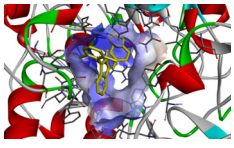	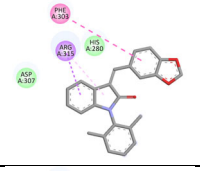
9	-9.8	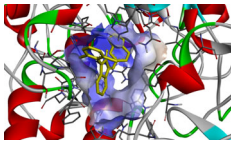	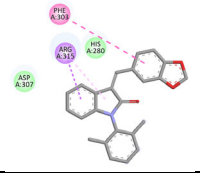

Table S4 Comparision of binding mode and binding energy of the most favourable ***Z*-5c**-3A4A complex.

Mode	Affinity (kcal mol^{-1})	Binding mode	
1	-10.9	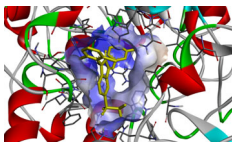	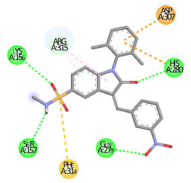
2	-10.9	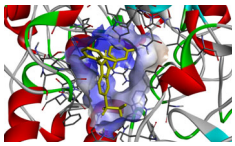	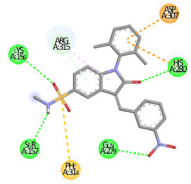
3	-10.5	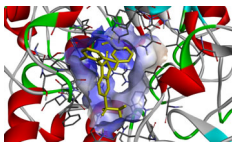	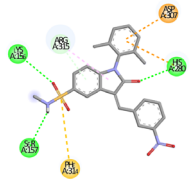
4	-10.4	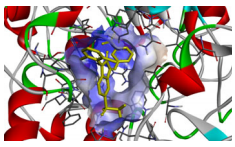	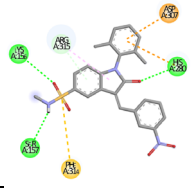
5	-10.2	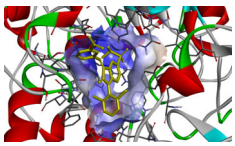	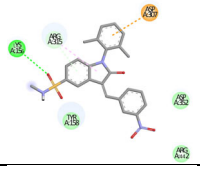
6	-10.2	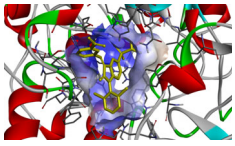	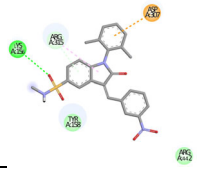
7	-10.2	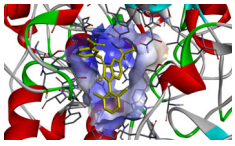	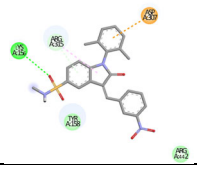
8	-10.0	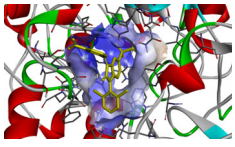	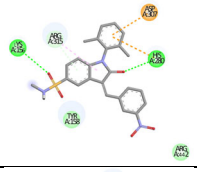
9	-9.6	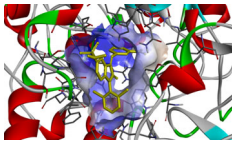	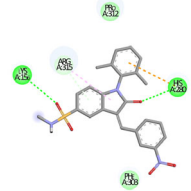

Table S5 Comparision of binding mode and binding energy of the most favourable *Z*-**5e**-3A4A complex.

Mode	Affinity (kcal mol^{-1})	Binding mode	
1	-10.9	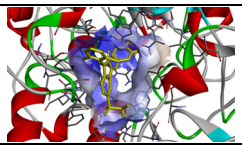	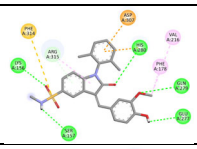
2	-10.9	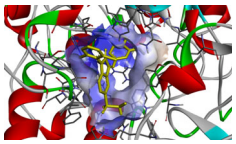	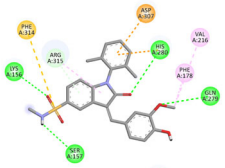
3	-10.4	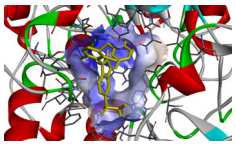	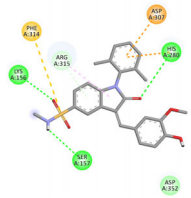
4	-10.4	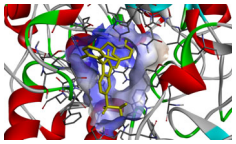	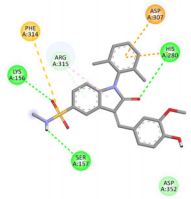
5	-9.9	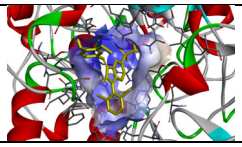	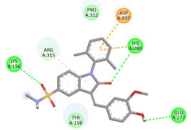
6	-9.9	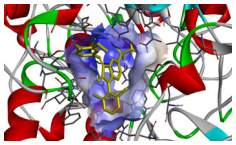	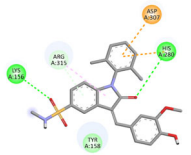
7	-9.3	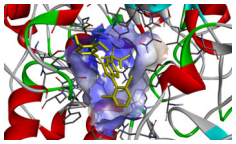	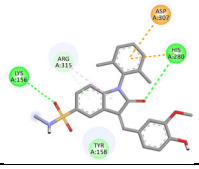
8	-9.3	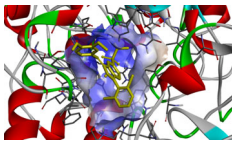	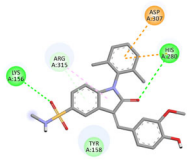
9	-9.1	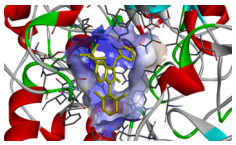	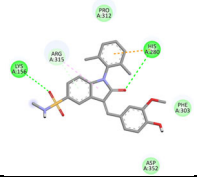

Table S6. Comparision of binding mode and binding energy of the most favourable *Z*-**5f**-3A4A complex.

Mode	Affinity (kcal mol^{-1})	Binding mode	
1	-10.9	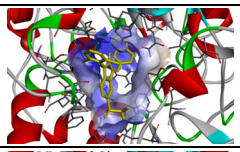	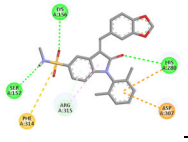
2	-10.9	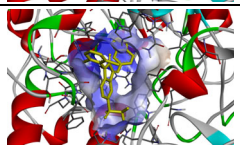	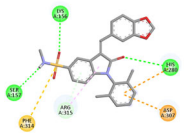
3	-10.7	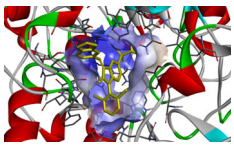	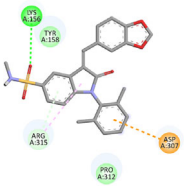
4	-10.7	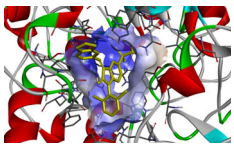	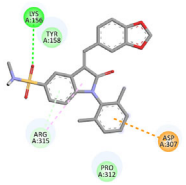
5	-10.4	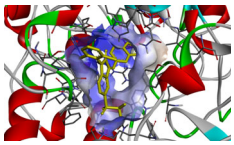	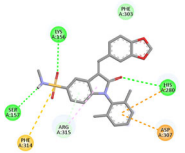
6	-10.2	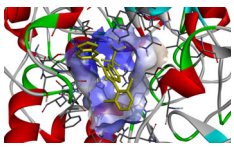	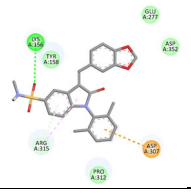
7	-10.1	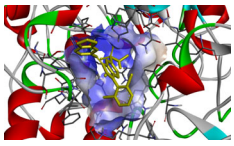	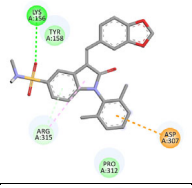
8	-10.0	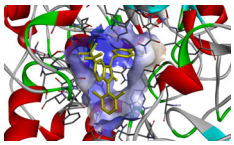	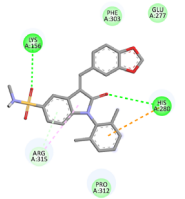
9	-9.6	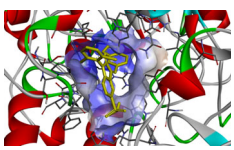	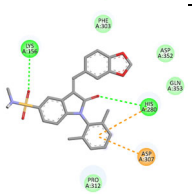

References

S1 H. Chen, X. Yan, W. Lin, L. Zheng and W. Zhang, *Pharm. Biol.*, 2004, **42**, 416.

S2 K. Yamamoto, H. Miyake, M. Kusunoki and S. Osaki, *FEBS J.*, 2010, **277**, 4205.